Article

Not peer-reviewed version

Anti-Tumor Effects of Cecropin A and Drosocin Incorporated into Macrophage-Like Cells Against Hematopoietic Tumors in *Drosophila mxc* Mutants

Marina Hirata , Tadashi Nomura , Yoshihiro H. Inoue *

Posted Date: 31 January 2025

doi: 10.20944/preprints202501.2343.v1

Keywords: *Drosophila* tumor; hemocytes; apoptosis; antimicrobial peptides (AMP); Phosphatidylserine; endocytosis

Article

Anti-Tumor Effects of Cecropin A and Drosocin Incorporated into Macrophage-Like Cells Against Hematopoietic Tumors in *Drosophila mxc* Mutants

Marina Hirata [1,2], Tadashi Nomura [1,2] and Yoshihiro H. Inoue [1]*

[1] Biomedical Research Center; [2] Graduate School of Science and Technology, Kyoto Institute of Technology

* Correspondence: yhinoue@kit.ac.jp; Tel.: +8175-7247876

Abstract: Five major antimicrobial peptides (AMPs) in *Drosophila* are induced in *multiple sex combs* (*mxc*) mutant larvae harboring lymph gland (LG) tumors and exhibit anti-tumor effects. The effects of the other well-known AMPs, Cecropin A and Drosocin, remain unelucidated. We investigated the tumor-elimination mechanism of these AMPs. A half-dose reduction of either *Toll* or *Imd* gene reduced the AMPs' induction in the fat body and enhanced tumor growth in mxc^{mbn1} mutant larvae, indicating that their anti-tumor effects depend on the innate immune pathway. Overexpression of these AMPs in the fat body suppressed tumor growth without affecting cell proliferation. Apoptosis was significantly promoted in the mutant LGs but not in normal tissues. Conversely, their knockdown inhibited apoptosis and enhanced tumor growth. Therefore, these AMPs inhibit LG tumor growth by inducing apoptosis. The AMPs from the fat body were incorporated into hemocytes of mutant but not normal larvae. Another AMP, Drosomycin, was taken up via phagocytosis factors. Enhanced phosphatidylserine signals were observed on the tumor surface. Inhibition of the cell-surface exposed signals impeded tumor growth suppression. AMPs may target phosphatidylserine in the tumors for apoptosis induction to execute tumor-specific effects. AMPs are potentially beneficial anti-cancer drugs with minimal side effects for clinical development.

Keywords: *Drosophila* tumor; hemocytes; apoptosis; antimicrobial peptides (AMP); Phosphatidylserine; endocytosis

1. Introduction

Insects such as *Drosophila* do not possess acquired immunity and thus rely on innate immunity for protection [1]. Although innate immunity provides only initial defense, its involvement in initiating and regulating acquired immunity has recently been reaffirmed [2,3]. Many studies on the molecular mechanisms of innate immunity have been conducted using *Drosophila*, since its specific functions are not overshadowed by the more powerful acquired immunity [4]. Thanks to advanced genetic and developmental biology methods, *Drosophila* offers an excellent model for studying immunity.

Innate immunity in *Drosophila* includes humoral and cellular defense responses [5,6,7]. Antimicrobial peptides (AMPs) play a major role in the humoral defense response. In response to infection, AMPs are produced by the fat body, whose functions are similar to those of the mammalian liver and adipose tissue [8]. AMP production is mediated by the activation of either, or both, of two major signaling pathways: Toll and Imd [1,8,9]. The Toll pathway is activated primarily by gram-positive bacteria or fungal infections [10,11]. Recognition proteins identify cell wall components common to those bacteria or fungi [12,13]. A serine protease cascade is then activated, ultimately producing an active Spätzle [14]. This binds to the Toll receptor, and the signals are transmitted into the cytoplasm [15]. Subsequently, the degradation of Cactus—which inhibits the nuclear translocation of the Dif and Dorsal transcription factors—translocates the factors into the nucleus and induces the transcription of relevant AMP genes [8,14]. In contrast, the Imd pathway is activated

 doi:10.20944/preprints202501.2343.v1

mainly by gram-negative bacterial infection [10]. The transmembrane receptor recognizes cell wall components common to these bacteria [16,17]. It then transmits signals via protein complexes including Imd [18,19]. Eventually, the Relish transcription factor allows its nuclear translocation and induction of the relevant AMP genes' transcription [16,20]. The *Drosophila* Toll- and Imd-mediated pathways are highly homologous to the mammalian Toll-like receptor and tumor necrosis factor (TNF) receptor-mediated signaling pathways, respectively [6,18,21]. Some of their target gene products, AMPs, are also conserved among different species. The first AMP, cecropin, was isolated in the 1980s from the silkworm moth, *Hyalophora cecropia* [22]. The following seven major AMPs are well characterized in *Drosophila*: Attacin, Cecropin, Defensin, Diptericin, Drosocin, Drosomycin, and Metchinikowin [1]. Among them, synthetic cecropin A peptides possess anti-tumor properties against cancer cells in culture systems [23,24,25]. AMP's cytotoxic and tumor growth-suppressive properties have been demonstrated *in vitro* as well as in *Drosophila* bodies [26,27,28,29]. Five of these seven AMPs are induced by activation of the innate immune pathway in response to tumors arising in imaginal discs and hematopoietic tissues, and effectively suppress tumor growth by inducing apoptosis in *Drosophila* [26,29]. However, it is still unclear how innate immunity recognizes tumor cells, how they activate the two innate immune pathways to induce AMPs, and how tumors are suppressed by AMPs from the fat body.

In *Drosophila*, mature hemocytes circulating in the hemolymph take charge of important innate immunity responses [30]. During the latter larval stage, hemocytes are supplied from the hematopoietic pockets and the lymph gland (LG). Plasmatocytes represent approximately 95% of hemocytes and act like macrophages, which eliminate apoptotic cells by phagocytosis. Hemocytes play a role in fighting bacterial infection as well as tumor cells by conveying immune signals toward the fat body to induce the expression of AMPs [31,32]. The transcriptional regulation of Drosocin via inter-tissue communication by hemocytes has been well characterized recently [31]. *Drosophila* hemocyte development and function are very similar to those of mammalian macrophages. Immune cell recruitment to tumor-forming foci is a hallmark of cancer [33]. *Drosophila* models also showed that hemocytes accumulate in tumors when they recognize damage to the basement membrane [34,35,36]. These cells produce Spätzle in tumors arising in the imaginal discs [28]. However, the detailed mechanisms of tumor recognition, signaling, and subsequent tumor suppression by hemocytes remain unelucidated.

The mxc^{mbn1} is a loss-of-function allele of the *multi sex combs* (*mxc*) gene and the hemizygotes for the mutation result in enlarged LG at the larval stage [26,37]. Moreover, mxc^{mbn1} exhibits a leukemia-like phenotype with increased numbers of undifferentiated hematopoietic cells in the hemolymph and their invasion to other tissues [38,39]. The LG tumors in the mxc^{mbn1} mutants exhibit overgrowth and invasive metastasis. In the mutant larvae, five of the seven major AMPs are induced and exhibit anti-tumor effects [26]. By contrast, two remaining AMPs, Cecropin A and Drosocin, have not been previously analyzed, although they are expected to be related to cancer and the innate immune system, as mentioned.

In this study, we focused on these two AMPs to determine whether they are induced in response to LG tumors and possess tumor-suppressive effects. We initially verified whether these AMP genes are induced in the fat body of mxc^{mbn1} mutants. We next examined whether the AMPs exhibit inhibitory effects on the LG tumors and suppress tumor growth by inducing apoptosis, as shown in the other five AMPs. Further, we address their anti-tumor effect mechanism in a tumor-specific manner. Our findings are expected to help elucidate the mechanisms of innate immune system activation and tumor suppression in response to *Drosophila* tumors. Although mammalian AMPs exhibit anti-cancer potential [40], most studies on their effects have been conducted in cultured cells. In contrast, our findings were determined using living organisms. This may benefit the future development of AMPs as promising new anti-cancer drugs with minimal side effects.

2. Materials and Methods

 doi:10.20944/preprints202501.2343.v1

2.1. Drosophila stocks

w^{1118} (*w*) was used as a normal control stock. The recessive lethal allele of *mxc*, mxc^{mbn1}, was used as a malignant hematopoietic tumor mutant [26,37,38,39]. The following Gal4 driver stocks were used for ectopic expression in specific larval tissues or cells as described; *w*; P{w+mC=r4-GAL4}3* for induction of gene expression in the fat body (#33832; Bloomington Drosophila Stock Center (BDRC) [26]), *P{He-GAL4.Z}85* (*He-Gal4*) (#8700; BDSC) for moderate induction in circulating hemocytes [37], *P{upd3-GAL4}* (a gift from N. Perrimon, Harvard Medical School, Boston, MA, USA) for induction of gene expression in LG tumor of mxc^{mbn1}. To monitor the gene expression of the *Dro*, *CecA* and *Drs* genes, *Dro-GFP* (a gift from M. Miura, University of Tokyo, Tokyo, Japan [40]), *CecA1-GFP* (#600216; BDSC [40]), and *Drs-YFP* (a gift from Y. Yagi, Nagoya University, Nagoya, Japan [41]) were used, respectively. To visualize the localization of Drosomycin in the circulating hemocytes, we used the *P{Drs-GFP.JM804}1* stock (#55707; BDSC) in which the EGFP-tagged Drosomycin expresses under its gene promoter. For dsRNA-dependent gene silencing, the following *UAS-RNAi* stocks were used; *P{GD498}v42503* (#42503; VDRC) (*UAS-DroRNAi*) [31], *P{GD3965}v9710* (#9710; VDRC) (*UAS-CecA1RNAi*) [42], *P{GD15912}* (#48383; VDRC) (*UAS-xkrRNAi*) [43], *P{w[+mC]=UAS-drpr.dsRNA}2* (*UAS-drprRNAi*) (#67034; BDSC) [44], and *P{TRiP.HMJ02128}attP40* (*UAS-sharkRNAi*) (#42555; BDSC). Those *UAS-RNAi* stocks could efficiently deplete the relevant mRNAs by combining them with Gal4 drivers. $P\{w^{+mC}$*=UAS-GFP.dsRNA.R}142* (#9330; BDSC) was used as a control for the *RNAi* experiments. To induce ectopic expression of the genes, the following *UAS* stocks were used; *UAS-Dro* and *UAS-CecA1* (respectively. gifts from B. Lemaitre, École Polytechnique Fédérale de Lausanne, Lausanne, Swiss [9,45]). For down-regulation of the innate immune pathways, imd^{1} and $Toll^{1\text{-}rxa}$ were used (a gift from Y. Yagi, Nagoya University, Nagoya, Japan [26]). For visualization of phosphoserine on the outside of the plasma membrane, *UAS-Annexin V-GFP* (a gift from C. Han, Cornell University, NY, USA [46]) was used.

All *Drosophila* stocks were maintained on standard cornmeal food, as previously described [47]. Per liter of water, 40 g of dried yeast (Asahi Group, Tokyo, Japan), 40 g of corn flour (Nippun, Tokyo, Japan), 100 g of glucose (Kato Chemical, Aichi, Japan), and 7.2 g of agar powder (Matsuki Agar, Nagano, Japan) were contained. 5 mL of 10 % methyl para hydroxybenzoate solution and 5 mL of propionic acid (Tokyo Kasei Kogyo, Tokyo, Japan) were added to 1 L of the fly food. Induction of Gal4-dependent gene expression was performed at 28°C. Other experiments and stock maintenance were conducted at 25°C.

2.2. Germline transformation

pUAST-CecA-CFLAGHA plasmid that permits cDNA expression for Cecropin A fused with FLAG- and HA- tags at its carboxyl-terminal under the UAS sequences (BDGF Tagged ORF collection, Drosophila Genomics Resource Center (Bloomington, Indiana, USA)). The plasmid DNA was injected into Drosophila embryos via PhiC31 integrase-mediated germ line transformation (BestGene Inc. (Chino Hills, CA, USA)).

2.3. Visualization of AMP gene expression in Drosophila larvae using Green fluorescent protein (GFP) reporter

Mature third instar larvae carrying the GFP reporters that monitored *Dro* and *CecA1* gene expression were collected and fixed on double-sided tape. The larvae were observed using a stereo fluorescence microscope SZX7 (OLYMPUS, Tokyo, Japan) equipped with a digital camera DIGITAL SIGHT DS-Fi2 (Nikon, Tokyo, Japan), and bright field images and fluorescent Images were acquired using the DS-L3 camera control unit (Nikon, Tokyo, Japan). A pair of fat body from mature third instar larvae was observed using a stereo fluorescence microscope SZX7 (OLYMPUS, Tokyo, Japan) equipped with a digital camera DIGITAL SIGHT DS-Fi2 (Nikon, Tokyo, Japan) and a camera control unit DS-L3 (Nikon, Tokyo, Japan) to obtain bright field and fluorescence images.

 doi:10.20944/preprints202501.2343.v1

2.4. Preparation of fixed samples to measure LG size

The *mxc*^{mbn1} was maintained heterozygous for the *FM7a, P{w[+mC]=sChFP}1* balancer. The larvae that did not express RFP were selected as the *mxc*^{mbn1} hemizygotes from the stock [26]. The larval LGs are attached along the dorsal vessel and have three lobe-like structures, which are paired on the left and right sides [48]. The first lobe contains mature hemocytes at the cortical zone, and undifferentiated hematopoietic precursors at the medullary zone [49,50]. Larval LGs collected from mature third-instar larvae were fixed in 4% paraformaldehyde for 15 minutes. DNA was stained with 4',6-diamidino-2-phenylindole (DAPI) solution (1 μg/ml in PBS (Wako Pure Chemicals, Osaka, Japan)). The LG specimen mounted under a mounting medium (Vector Laboratories, CA, USA) was gently spread to obtain a single LG cell layer as described elsewhere [26]. To quantify the size of DAPI-stained LG, the entire area of each hemisphere of the LG was measured on the acquired fluorescence image using Image J software (https://imagej.nih.gov/ij/).

2.5. LG immunostaining

The fixed LG samples were blocked with PBS containing 0.1% Triton X-100 and 10% normal goat serum and incubated with the primary antibodies (anti-cDcp1 (Asp215) antibody (1:500; #9578, Cell Signaling Technology, Danvers, MA, USA) and anti-PH3(Ser10) antibody (1:1000; #06-570, Merk-Millipore, MA, USA)) overnight at 4°C. After washing repeatedly, the secondary antibody conjugated with Alexa Fluor 488 (1:400; #A11008, Molecular Probes, OR, USA) was added to detect the primary antibodies. DAPI was used for the DNA staining. The stained LG samples mounted in VECTASHIELD Mounting Medium (Vector Laboratories, CA, USA) were observed with an inverted fluorescence microscope IX81 (OLYMPUS, Tokyo, Japan) equipped with a digital CCD camera ORCA-R2 (Hamamatsu Photonics, Shizuoka, Japan). Fluorescence images were acquired using MetaMorph® 7.6 Software (Molecular Devices, CA, USA) and then processed on Adobe Photoshop CS (Adobe, CA, USA). The areas emitting the immunofluorescent signals among each hemisphere of the LG were measured on the fluorescence images by Image J. The percentage of the fluorescence areas in the anterior LG lobes was calculated.

2.6. Detection of Phosphatydilserine (PS) exposed on the cell membrane surface in LG

To detect PS on the surface of LG cells, GFP-tagged Annexin V—which binds to PS at a high affinity—was expressed in the fat body using the *r4-Gal4* driver. When we observe the PS on the LGs of the larvae harboring the precursor cells-specific depletion of *xkr* mRNA using the *upd3-Gal4* driver, Annexin V-GFP expression via the simultaneous use of *r4-Gal4* cannot be induced. Thus, larval LGs collected from mature third instar larvae were incubated with 5% Alexa Fluor 594-conjugated Annexin V (#A13203, Life Technologies, CA, USA) for 30 min. The LGs were fixed in 4% paraformaldehyde for 15 min. DAPI-staining and fluorescence imaging were then carried out as described above. The GFP fluorescence-positive areas among the anterior lobes of each LG hemisphere on the fluorescence images were measured using Image J. The percentage of the fluorescence areas in the whole LG lobe region was calculated.

2.7. Immunostaining of circulating hemocytes

A single larva at the third instar stage was transferred into the *Drosophila* Ringer's solution (DR) on a glass slide. Subsequently, only the larval epidermis was cut using a set of fine forceps to allow the circulating hemocytes to be released into the DR outside the larvae. After an aliquot of the DR containing circulating hemocytes was placed on the glass slide, the hemocytes were fixed in 4% paraformaldehyde for 10 min. Immunostaining of the hemocytes was performed using anti-HA-tag rabbit IgG (1:1000; #3724, Cell Signaling Technology, Danvers, MA, USA) as described above. Fluorescence intensities of the hemocytes were quantified using Image J.

2.8. Microinjection of synthetic cecropin A peptides

 doi:10.20944/preprints202501.2343.v1

A 50 μM solution of synthetic cecropin A (#C6830, Sigma-Aldrich, St. Louis, USA) dissolved in DR containing a red food color was prepared for microinjection [51]. Using red pigment as an injection marker, approximately 0.1 μL of the AMP solution was injected into the posterior-ventral area of a recipient larva at the third instar, using glass needles. The needles were prepared from G1.2 capillaries (outer diameter of 1 mm, Narishige Co., Tokyo, Japan) using a grass puller (PN-31, Narishige Co., Tokyo, Japan). They were ground against the side of the microscope glass to sharpen the tip. After injection, the larvae were placed on a piece of wet filter paper for 1 hour to recover from the damage and raised on standard food overnight before observation.

2.9. Quantitative reverse transcription-PCR (qRT-PCR) analysis

Total RNA was extracted from 14 to 18 pairs of fat bodies of mature third instar larvae using Trizol Regent® (Invitrogen, USA, MA). After treatment with DNase I (Epicentre Technologies, WI, USA) to remove mixed genomic DNA, the purity of RNA was checked by ensuring that the A260 and A280 ratio of each RNA sample was between 1.8 and 2.0. cDNA was synthesized from the total RNA using a PrimeScript High-Fidelity RT-PCR Kit (TaKaRa, Clontech Laboratories, Shiga, Japan). Real-time PCR reactions were performed on a Thermal Cycler Dice® Real-Time System III (TaKaRa Bio, Shiga, Japan) using TB Green® Premix Ex Taq™ II Tli RNaseH Plus (TaKaRa Bio, Shiga, Japan). The PCR reaction was carried out using a cycling program consisting of initial denaturation at 95°C for 5 m, followed by 40 cycles at 95°C for 5 s and 60°C for 30 s. The temperature was increased from 60°C to 95°C at a rate of 0.1°C/s. Real-time PCR was performed using a Thermal Cycler Dice® Real-Time System III (TaKaRa Bio., Shiga, Japan) using TB Green Premix Ex Taq II (#RR820A, TaKaRa Bio, Shiga, Japan). Each sample was analyzed in triplicate on a PCR plate, and the final results were obtained by averaging three biological replicates. For quantification, the ΔΔCt method was used to determine the differences between target gene expression and that of the reference gene, Rp49. Three identical PCR reaction reagents were prepared for one cDNA sample, and the mean and standard deviation of mRNA amounts were calculated. mRNA amounts were analyzed by the ΔΔCt method. The following primer sequences were used in the real-time quantitative PCR; RP49-Fw, 5′-TTCCTGGTGCACAACGTG-3′ and RP49-Rv, 5′-TCTCCTTGCGCTTCTTGG-3′; Cecropin A1-Fw, 5′-TCTTCGTTTTCGTCGCTCTC-3′ and Cecropin A1-Rv, 5′-CTTGTTGAGCGATTCCCAGT-3′; Drosocin-Fw, 5′-TCAGTTCGATTTGTCCACCA-3′ and Drosocin-Rv, 5′-GATGGCAGCTTGAGTCAGGT-3′.

2.10. Statistical analysis

Welch's *t-test* and one-way ANOVA for multiple comparisons were used to assess statistical differences. Unless otherwise stated, one-way ANOVA multiple comparison with Bonferroni correction was used for statistical comparisons. Sample sizes and *p*-values are given in the description of the results. A *p*-value of 0.05 or less was considered statistically significant. The results of each tabulation were displayed as scatter plots or bar charts created using GraphPad Prism 6 (GraphPad Software, CA, USA).

3. Results

3.1. Induction of AMP genes encoding Drosocin and Cecropin A in the fat body of mxc^{mbn1} mutant larvae

Transcription of genes encoding the five major AMPs was induced in the fat body of mxc^{mbn1} mutant larvae [26]. Thus, we first examined whether the other two major AMP genes encoding Drosocin (*Dro*) and Cecropin A (*CecA1*) showed a consistent induction of transcription in the mutant fat body. First, we visualized *Dro* gene expression in the fat body of normal (*w/Y; Dro-GFP/+*) and mxc^{mbn1} mutant larvae (mxc^{mbn1}*/Y; Dro-GFP/+*) at the third instar stage using the green fluorescent protein (GFP) reporter. GFP fluorescence was not detected in the normal control (n = 20) (**Figure 1**a′). In contrast, the mxc^{mbn1} larvae (n = 23) showed GFP fluorescence in the fat body of 35% (n = 8/23) of the larvae (**Figure 1**b′), although the fluorescence intensity was weaker than that observed in bacterial

 doi:10.20944/preprints202501.2343.v1

infection. Similarly, *CecA1* gene expression in the fat body of third-instar mature larvae of normal controls (*w/Y; CecA1-GFP/+*) and *mxc*^{mbn1} mutants (*mxc*^{mbn1}*/Y; CecA1-GFP/+*) was visualized using the GFP reporter. GFP fluorescence was not detected in the controls (n = 20) (**Figure 1**c′) but was detected in the fat body of 33% (n = 11/33) of the mutant larvae at the same stage (**Figure 1**d′). These findings suggest that the *Dro* and *CecA1* genes were upregulated in the fat body of *mxc*^{mbn1} larvae.

To confirm the upregulation of *Dro* and *CecA1* in *mxc*^{mbn1} larvae, we performed quantitative reverse transcription-PCR (qRT-PCR) experiments using total RNA from the fat body of the normal control (*w/Y*) and mutant (*mxc*^{mbn1}*/Y*) larvae at the third instar mature stage. *Dro* mRNA levels were significantly elevated by approximately 50-fold in the mutant fat body compared to those of the normal controls ($p < 0.05$) (**Figure 1**e). The average mRNA levels of *CecA1* increased approximately 7-fold, respectively, in the mutants compared to those in the normal controls (**Figure 1**f). Thus, the *Dro* and the *CecA1* genes were overexpressed in the fat body of *mxc*^{mbn1} larvae harboring the LG tumor.

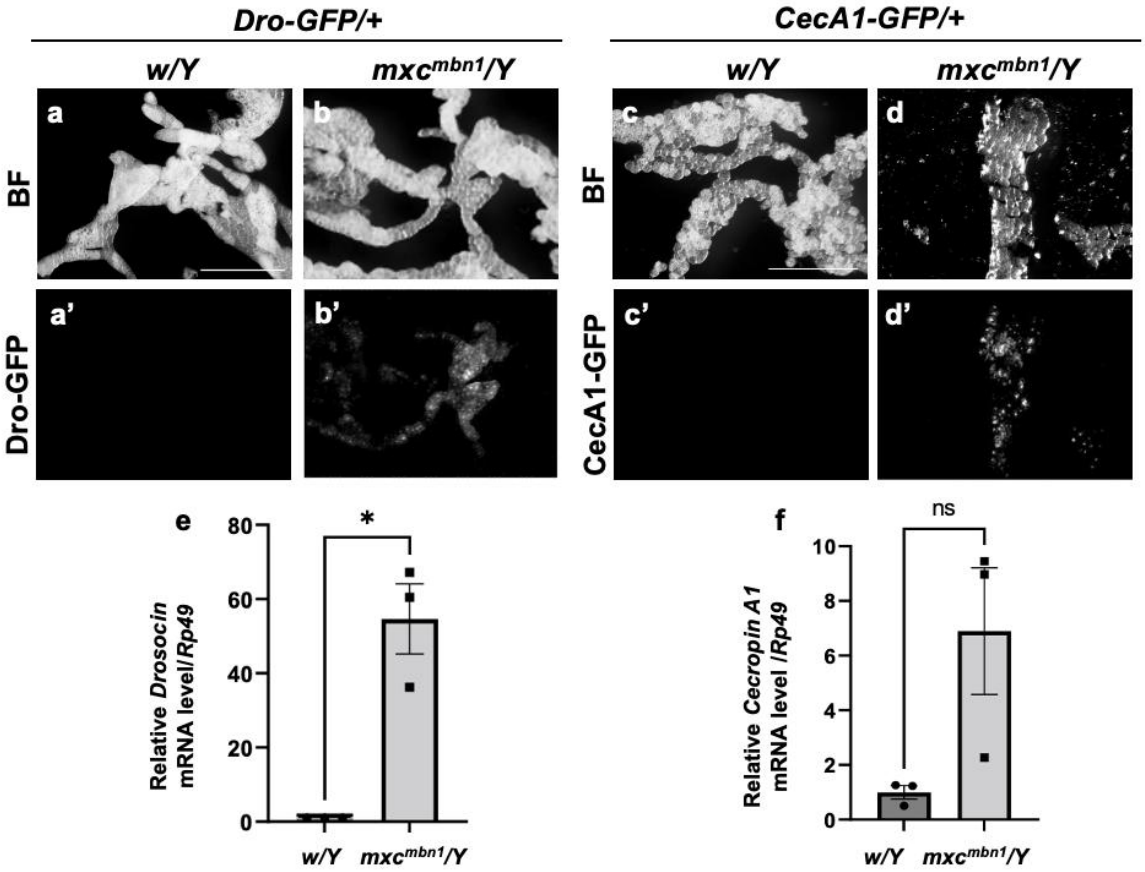

Figure 1. Expression of *Dro-GFP* and *CecA1-YFP* reporters in the fat body of *mxc*^{mbn1} mutant larvae. (**a**, **b**) Bright-field (BF) stereomicroscopic images of the fat body of third instar mature larva carrying the *Drosocin* (*Dro*)*-GFP* reporter. Scale bars: 500 μm. (**a′**, **b′**) Green fluorescent protein (GFP) fluorescence images in the fat body of third instar mature larvae with *Dro-GFP* reporter. (**c**, **d**) BF stereomicroscopic images of the fat body in a third instar mature larva carrying the *Cecropin A1* (*CecA1*)*-GFP* reporter. (**c′**, **d′**) GFP fluorescence images in the fat body of the larvae with *CecA1-GFP* reporter. (**a**, **c**) Normal control (*w/Y*) and (**b**, **d**) *mxc*^{mbn1} mutant (*mxc*^{mbn1}*/Y*) larvae. (**e**, **f**) mRNA quantification of *Dro* and *CecA1* using quantitative reverse transcription-PCR (qRT-PCR). The X-axis of each graph shows the mRNA levels of the normal control (*w/Y*) and *mxc*^{mbn1} (*mxc*^{mbn1}*/Y*) larvae from left to right; the Y-axis shows the mRNA levels of the target gene relative to the endogenous control gene (*Rp49*). (**e**, **f**) mRNA levels of the *Dro* (**e**) and *CecA1* (**f**) genes. Welch's *t*-test assessing each experimental group (*$p < 0.05$, ns: not significant).The error bars indicate the standard error of the mean (SEM).

 doi:10.20944/preprints202501.2343.v1

3.2. Dro and CecA1 mRNA level declines and LG hyperplasia enhancement in mxc^{mbn1} larvae by half-dose reduction of the genes encoding the innate immune pathway factors

We investigated whether *Dro* and *CecA1* in *mxc^{mbn1}* were induced via the activation of innate immune pathways. Genetic analysis was performed to determine the reduction in gene expression and its influence on LG tumor size when the innate immunity pathway was downregulated. Heterozygotes for *Toll* or *imd* mutations in *mxc^{mbn1}* mutants exhibited reduced mRNA levels of the five other AMP genes [26]. In *mxc^{mbn1}* mutants heterozygous for a loss-of-function mutation for *Toll* (*mxc^{mbn1}/Y; Toll$^{1\text{-}RXA}$/+*) or *imd* (*mxc^{mbn1}/Y; imd/+*), the mRNA levels of *Dro* and *CecA1* in the fat body were quantified using qRT-PCR with RNA prepared from the fat body of third instar stage larvae. The *Dro* mRNA level declined to approximately 7% of that of *mxc^{mbn1}* (*mxc^{mbn1}/Y*) in the mutant larvae heterozygous for the *Toll* mutation and to approximately 3% in *imd* heterozygous mutants (**Figure S1**a). These differences were statistically significant ($p < 0.0001$). Consistently, the *CecA1* mRNA levels declined to 35% of those of *mxc^{mbn1}* in the mutant larvae heterozygous for the *Toll* mutation and by approximately one-third in *imd* heterozygous mutants (**Figure S1**b). This difference was statistically significant ($p < 0.01$).

Next, we observed whether the growth of the LG tumor was enhanced when the mRNAs of AMP genes were downregulated in *mxc^{mbn1}* heterozygous for the *Toll* or *imd* mutation (**Figure S1**c-f). The entire LG lobe region size in mature larvae at the third instar stage was quantified. LG tumor size (mean: 0.55 mm^2, n = 20) increased significantly by 1.13-fold in *mxc^{mbn1}* larvae heterozygous for *Toll* mutation compared to those in *mxc^{mbn1}* larvae without the mutation (mean: 0.48 mm^2, n=20) (**Figure S1**g) ($p < 0.05$). Consistently, the LG tumors in *mxc^{mbn1}* heterozygous for the *imd* mutation (mean: 0.67 mm^2, n = 20) were 1.38-fold larger (**Figure S1**g) than those in *mxc^{mbn1}* (mean: 0.48 mm^2, n = 20). This difference was statistically significant ($p < 0.0001$). In summary, LG hyperplasia was enhanced in *mxc^{mbn1}* mutants heterozygous for *Toll* or *imd* mutations. Thus, LG tumors may be suppressed by the gene products of *Dro* and *CecA1* induced by innate immune pathway activation.

3.3. LG hyperplasia suppression in mxc^{mbn1} larvae by overexpression of Dro or CecA1 gene in the fat body

Further, we investigated the anti-tumor potential of Drosocin and Cecropin A. The fat body-specific overexpression of either gene (*w/Y; r4>Dro* or *w/Y; r4>CecA1*) did not affect LG size, relative to that of normal control larvae (*w/Y; r4>+*) (**Figure 2**a-c). We next compared the LG size of *Dro*-overexpressing *mxc^{mbn1}* larvae in the fat body (*mxc^{mbn1}/Y; r4>Dro*) with that of *mxc^{mbn1}* larvae (*mxc^{mbn1}/Y; r4>+*) (**Figure 2**d, e). The average size of the entire LG lobe region (mean: 0.18 mm^2, n = 20) was significantly reduced to approximately one-third of that of *mxc^{mbn1}* (mean: 0.48 mm^2, n = 20) (**Figure 2**g) ($p < 0.0001$). These results indicate the anti-tumor potential of Drosocin on LG tumors in *mxc^{mbn1}*. Next, we compared the LG size of *mxc^{mbn1}* larvae with fat body-specific *CecA1* overexpression (*mxc^{mbn1}/Y; r4>CecA1*) to that of *mxc^{mbn1}* larvae (*mxc^{mbn1}/Y; r4>+*) (**Figure 2**d, f). The LG size (mean: 0.15 mm^2, n = 20) was significantly reduced to approximately one-third of that of the control (*mxc^{mbn1}/Y; r4>+*) (mean: 0.48 mm^2, n = 20) (**Figure 2**g) ($p < 0.0001$). These results indicate the anti-tumor potentials of Drosocin and Cecropin A, which suppressed LG tumor growth in *mxc^{mbn1}* larvae.

 doi:10.20944/preprints202501.2343.v1

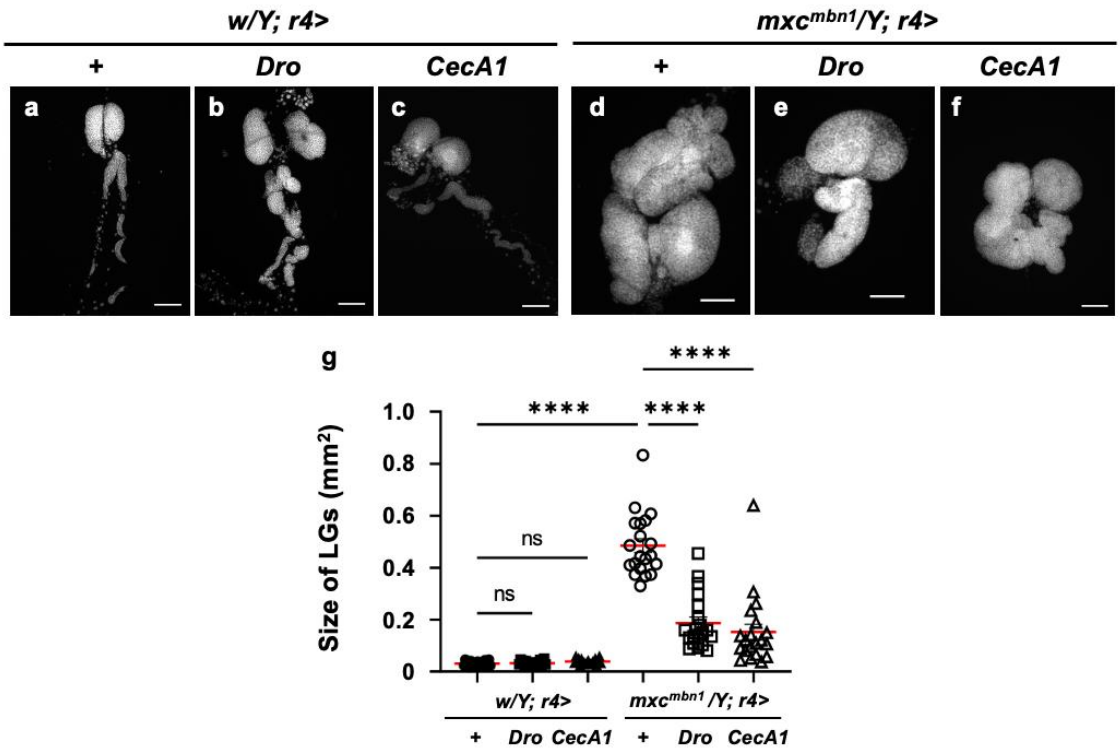

Figure 2. Observation of lymph glands (LGs) from *mxc*^{mbn1} larvae and quantification of their size by induction of *Dro* or *CecA1* overexpression in a fat body (FB)-specific manner. (**a**-**f**) Fluorescence images of DAPI-stained LGs collected from mature third instar larvae. (**a**) Pair of LGs from a normal control larva (*w/Y; r4>+*). (**b**) LG from control larvae with FB-specific overexpression of *Dro* (*w/Y; r4>Dro*) or (**c**) *CecA1* (*w/Y; r4>CecA1*). A pair of LGs from (**d**) *mxc*^{mbn1} larva (*mxc*^{mbn1}*/Y; r4>+*), (**e**) *mxc*^{mbn1} larvae with FB-specific expression of *Dro* (*mxc*^{mbn1}*/Y; r4>Dro*) or (**f**) *CecA1* (*mxc*^{mbn1}*/Y; r4>CecA1*). Scale bars: 100 μm. (**g**) LG size quantification in larvae with FB-specific expression of *Dro* (*w/Y; r4>+* (n = 20), *w/Y; r4>Dro* (n = 20), *mxc*^{mbn1}*/Y; r4>+* (n = 20), *mxc*^{mbn1}*/Y; r4>Dro* (n = 20)), and *CecA1* ((*w/Y* (n = 20), *w/Y; r4>CecA1* (n = 20), *mxc*^{mbn1}*/Y; r4>+* (n = 20), *mxc*^{mbn1}*/Y; r4>CecA1* (n = 20)). Differences between each experimental group were performed using one-way ANOVA for multiple comparisons (****p < 0.0001, ns: not significant). The red lines indicate the mean LG size. The error bars indicate the SEM.

3.4. Dro or CecA1 overexpression in the fat body enhanced apoptosis in the LG tumors of mxc^{mbn1} *larvae*

To elucidate the mechanism underlying the anti-tumor effect of Drosocin and Cecropin A, we investigated whether these two AMPs exhibit apoptosis-inducing effects in LG tumors, similar to those of the other five AMPs [26]. First, we confirmed that fat body-specific overexpression of *Dro* (*w/Y; r4>Dro*) or *CecA1* (*w/Y; r4>CecA1*) did not influence LG size in normal larvae. The percentage of anti-cDcp1 immunostaining signal-positive area in the total lobe region of the LG was calculated and compared to that of the control (*w/Y; r4>+*) (**Figure 3**a'-c'). Next, we performed anti-cDcp1 immunostaining of the LG in *mxc*^{mbn1} mutant larvae harboring fat body-specific overexpression of *Dro* (*mxc*^{mbn1}*/Y; r4>Dro*). LGs of the third instar larvae showed an immunostaining signal corresponding to apoptotic cells in an average of 22.1% (n = 21) of the total lobe area (n = 21), which was significantly (1.8-fold) higher than the average of 12.9% (n = 20) in the control (*mxc*^{mbn1}*/Y; r4>+*) (**Figure 3**d', e', g) (p < 0.05). These results suggest that Drosocin induces apoptosis in *mxc*^{mbn1} mutant LG tumors. Consistently, fat body-specific overexpression of *CecA1* in *mxc*^{mbn1} larvae (*mxc*^{mbn1}*/Y; r4>CecA1*) also significantly increased the apoptosis area in an average of 29.4% of the total lobe area of LGs (n = 24) in third instar stage larvae. This percentage was 2.3-fold higher than the average of 12.9% (n = 20) in controls (*mxc*^{mbn1}*/Y; r4>+*) (**Figure 3**d', f', g) (p < 0.0001). These results suggest that Cecropin A could induce apoptosis in *mxc*^{mbn1} mutant LG tumors.

To further confirm whether the apoptosis induction occurs in tumor-specific manner, we overexpressed *Dro* or *CecA1* specifically in the fat body of normal larvae and investigated apoptosis

 doi:10.20944/preprints202501.2343.v1

in larval tissues such as imaginal discs by anti-cDcp1 immunostaining. Consequently, few signals were observed in wing imaginal discs, similar to the controls (**Figure S2**a-c). Thus, Drosocin and Cecropin A induced apoptosis specifically in the LG tumors of *mxc*^{mbn1} larvae.

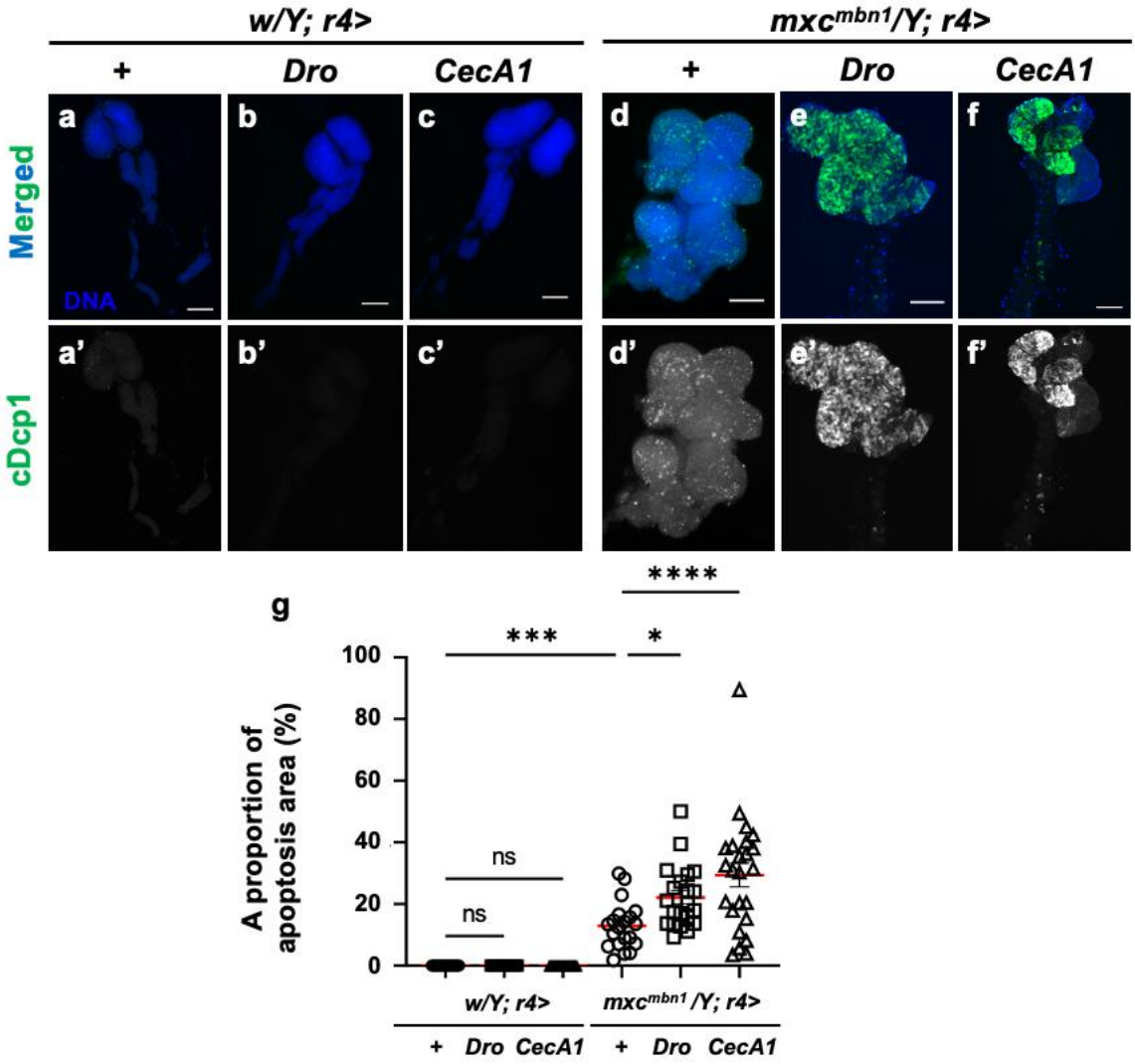

Figure 3. Observation and quantification of apoptosis areas in LGs of *mxc*^{mbn1} larvae harboring fat body (FB)-specific overexpression of *Dro* or *CecA1*. (**a**-**f**) Immunostaining of LGs with anti-cDcp1 antibodies that recognize apoptotic cells in LGs from the third instar-stage mature larvae. (**a**) A pair of LGs from control larvae (*w/Y; r4>+*). (**b**) Control larvae overexpressing *Dro* (*w/Y; r4>Dro*), or (**c**) *CecA1* (*w/Y; r4>CecA1*) specifically in the FB. (**d**) Anterior lobes of a pair of LGs from *mxc*^{mbn1} larvae (*mxc*^{mbn1}*/Y; r4>+*). (**e**) *mxc*^{mbn1} larvae overexpressing *Dro* (*mxc*^{mbn1}*/Y; r4>Dro*) or **(f)** *CecA1* (*mxc*^{mbn1}*/Y; r4>CecA1*). Blue indicates DNA staining; green indicates anti-cDcp1 immunostaining signals. Scale bars: 100 μm. (**g**) Percentage of areas occupied by apoptotic cells in the lobe regions of LGs from larvae with FB-specific *Dro* overexpression (n = 21 LGs from 11 larvae) or *CecA1* (n = 24 LGs from 12 larvae). One-way ANOVA multiple comparisons (*$p < 0.05$, ***$p < 0.001$, ****$p < 0.0001$, ns: not significant). The red line indicates the mean percentage of apoptosis. The error bars indicate the SEM.

3.5. Dro or CecA1 knockdown in the fat body enhanced LG hyperplasia and suppressed apoptosis in LG tumors in mxc^{mbn1} *larvae*

We next investigated whether these two AMPs exhibited an anti-tumor effect. We induced dsRNA against *Dro* mRNA (*w/Y; r4>DroRNAi*) or dsRNA against *GFP* mRNA in the fat body of normal controls (*w/Y; r4>GFPRNAi*) (**Figure 4**a, b). The average LG tumor sizes of these controls were

 doi:10.20944/preprints202501.2343.v1

0.032 mm² (n = 20) and 0.031 mm² (n = 21), respectively (**Figure 4**g). No significant differences were observed. Further, we compared LG size between *mxc*^{mbn1} larvae harboring fat body-specific *Dro* depletion (*mxc*^{mbn1}*/Y; r4>DroRNAi*) and *mxc*^{mbn1} mutant larvae expressing non-specific dsRNA against GFP mRNA (*mxc*^{mbn1}*/Y; r4> GFPRNAi*) (**Figure 4**d, e). The average size of the LG lobe area in mutant larvae harboring the *Dro* depletion (mean: 0.51 mm², n = 15) was significantly larger (1.43 times) than that in the controls (mean: 0.36 mm², n = 12) (**Figure 4**g) ($p < 0.001$). These results indicated the anti-tumor effect of Drosocin, which suppressed LG tumor growth in *mxc*^{mbn1}.

Consistently, fat body-specific depletion of *CecA1* (*w/Y; r4>CecA1RNAi*) or ectopic expression of non-specific dsRNA against GFP mRNA (*w/Y; r4>GFPRNAi*) did not significantly affect LG size in normal larvae (**Figure 4**a, c). We compared the LG size of *mxc*^{mbn1} larvae harboring fat body-specific depletion of *CecA1* (*mxc*^{mbn1}*/Y; r4>CecA1RNAi*) with that of *mxc*^{mbn1} mutants expressing dsRNA against GFP mRNA (*mxc*^{mbn1}*/Y; r4> GFPRNAi*) (**Figure 4**d, f). The area of the entire LG lobe region in the mutant larvae harboring the depletion of *CecA1* (mean: 0.48 mm², n = 13) was larger (1.34 times) than that of the controls (mean: 0.36 mm², n = 12) (**Figure 4**g) ($p < 0.01$). These results indicate that Cecropin A also has an anti-tumor effect on *mxc*^{mbn1} LG tumors.

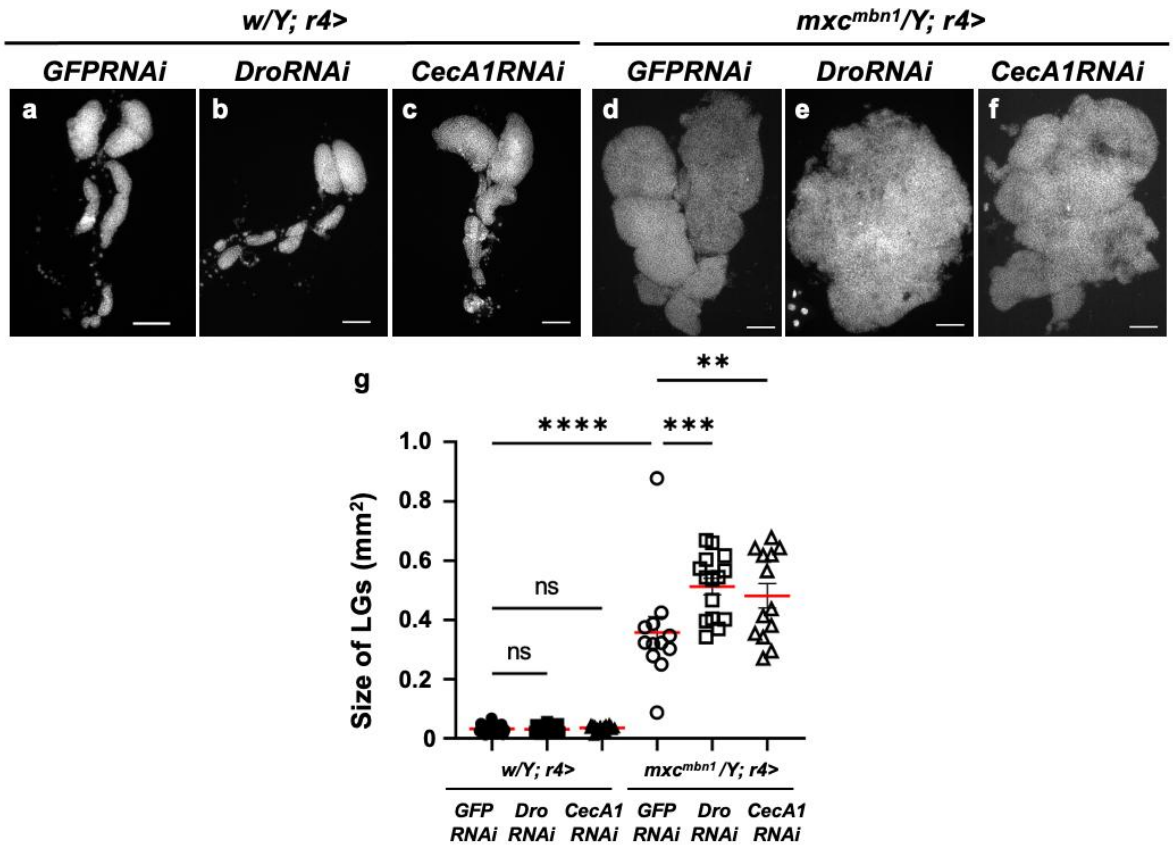

Figure 4. Quantification of LG sizes in *mxc*^{mbn1} larvae harboring FB-specific knockdown of *Dro* or *CecA1*. (**a**-**f**) DAPI-stained images of LGs from mature third instar stage larvae. (**a**-**c**) LGs expressing dsRNAs against mRNAs for (**a**) *GFP* (*w/Y; r4>GFPRNAi*) (control), (**b**) *Dro* (*w/Y; r4>DroRNAi*), or (**c**) *CecA1* (*w/Y; r4>CecA1RNAi*) specifically in the fat body are shown. (**d**-**f**) LGs expressing dsRNAs against (**d**) *GFP* in the fat body of *mxc*^{mbn1} larvae (*mxc*^{mbn1}*/Y; r4>GFPRNAi*), (**e**) *Dro* (*mxc*^{mbn1}*/Y; r4>DroRNAi*) or (**f**) *CecA1* (*mxc*^{mbn1}*/Y; r4>CecA1RNAi*). Scale bars: 100 μm. (**g**) Quantification graphs of the LG size that larvae of each genotype have. The LG size of larvae with *DroRNAi* (n = 15 LGs from 8 larvae) and *CecA1RNAi* (n = 13 LGs from 7 larvae). One-way ANOVA multiple comparisons (**$p < 0.01$, ***$p < 0.001$, ****$p < 0.0001$, ns: not significant). The red lines indicate the mean LG size. The error bars indicate the SEM.

 doi:10.20944/preprints202501.2343.v1

To further confirm apoptosis induction in mutant LGs by *Dro* or *CecA1* overexpression, we investigated whether their depletion influenced LG tumors. First, we confirmed that neither depletion of *Dro* mRNA (*w/Y; r4>DroRNAi*) nor ectopic expression of non-specific dsRNA against *GFP* mRNA (*w/Y; r4>GFPRNAi*) in the fat body influenced a positive area stained with anti-cDcp1 antibody in LGs of normal larvae (**Figure 5**a', b'). In mxc^{mbn1} larvae harboring fat body-specific expression of dsRNA against *GFP* mRNA, we observed anti-cDcp1 immunostaining signal in an average of 17.7% of the total lobe areas (n = 12) in the mutant LG in third instar larvae (mxc^{mbn1}/*Y; r4>GFPRNAi*). In contrast, in the LGs of the mutant larvae harboring fat body-specific depletion of *Dro* (mxc^{mbn1}/*Y; r4>DroRNAi*), we observed an average of 6.2% of the total lobe areas (n = 15) (**Figure 5**d, e). This percentage declined to 35% of that in the LGs of mutant larvae harboring the non-specific dsRNA expression (**Figure 5**g) ($p < 0.0001$). These results indicate that Drosocin induces apoptosis in LG tumors in mxc^{mbn1} mutant larvae.

Next, we also confirmed whether *CecA1* depletion in the fat body suppressed apoptosis in the mutant LGs. We confirmed that neither depletion of *CecA1* mRNA (*w/Y; r4>CecA1RNAi*) nor ectopic expression of non-specific dsRNA against *GFP* mRNA (*w/Y; r4>GFPRNAi*) in the fat body influenced apoptosis areas in the LGs of normal larvae (**Figure 5**a', c'). In contrast to the average percentage of 17.7% (n = 12) in the mutant LGs, (mxc^{mbn1}/*Y; r4>GFPRNAi*), we observed the apoptosis signals in an average 9.3% (n = 13) of the total lobe area in the LGs of the mutant larvae at the same third instar stage (**Figure 5**d, f). This percentage declined by approximately 50% in the LGs of mutant larvae harboring the non-specific dsRNA expression (**Figure 5**g) ($p < 0.0001$). These results indicate that Cecropin A induced apoptosis in the LG tumors of mxc^{mbn1} larvae.

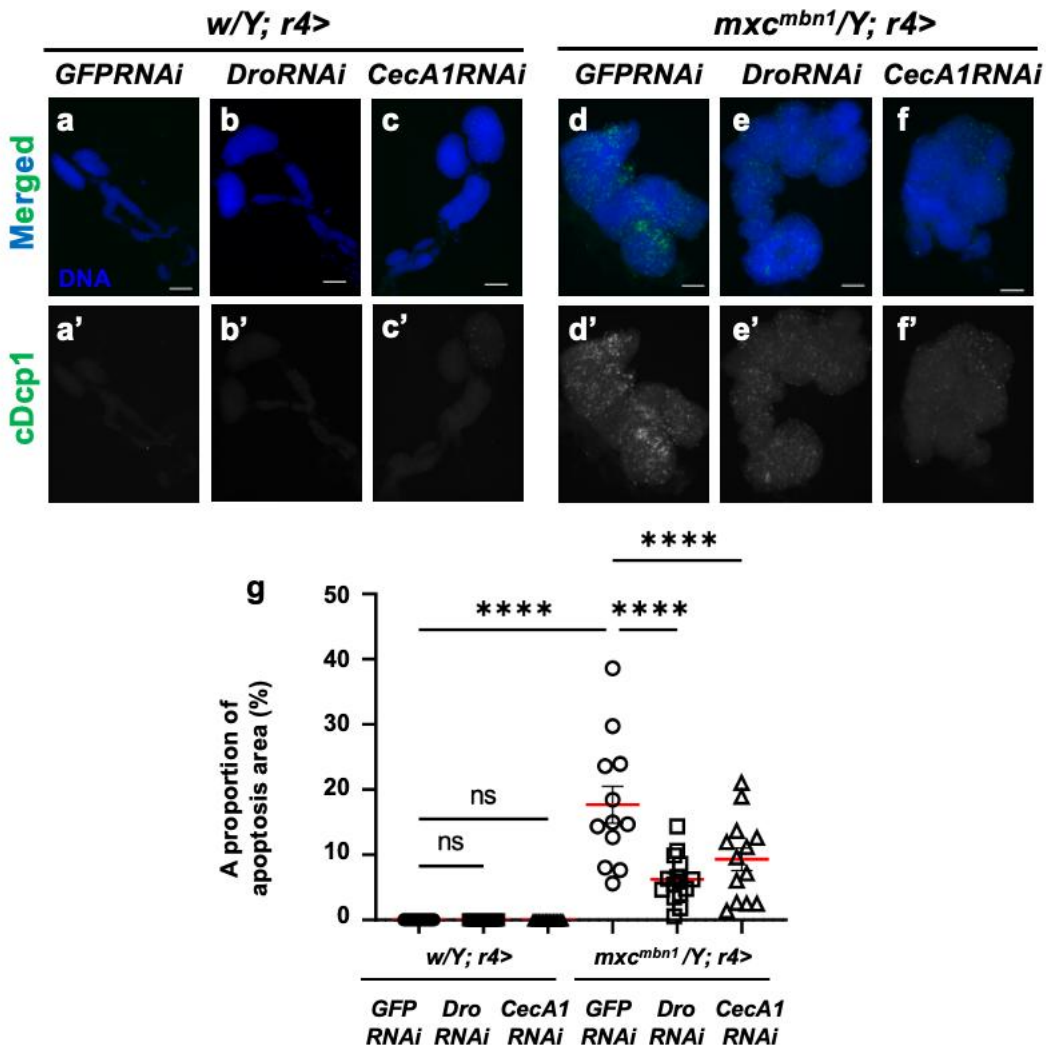

 doi:10.20944/preprints202501.2343.v1

Figure 5. Apoptosis observation and quantification in LGs of *mxc*^{mbn1} larvae harboring fat body-specific knockdown of *Dro* or *CecA1*. (**a**-**f**) Immunostaining of LGs with anti-cDcp1 antibodies that recognize apoptotic cells. LGs expressing dsRNA against mRNAs for (**a**) *GFP* (*w/Y; r4>GFPRNAi*), (**b**) *Dro* (*w/Y; r4>DroRNAi*), or (**c**) *CecA1* (*w/Y; r4>CecA1RNAi*) specifically in the fat body are shown. (**d**-**f**) LG expressing dsRNA against (**d**) *GFP* specifically in the fat body of *mxc*^{mbn1} larvae (*mxc*^{mbn1}*/Y; r4>GFPRNAi*), (**e**) *Dro* (*mxc*^{mbn1}*/Y; r4>DroRNAi*) or (**f**) *CecA1* (*mxc*^{mbn1}*/Y; r4>CecA1RNAi*) are shown. Blue indicates DNA staining; green indicates an anti-cDcp1immunostaining signal. Scale bars: 100 μm. (**g**) The graphs indicate the percentage of apoptotic cells in the lobe regions of the LGs of larvae harboring FB-specific depletion of *Dro* (n = 15 LGs from 8 larvae) or *CecA1* (n = 13 LGs from 7 larvae). One-way ANOVA multiple comparisons (****$p < 0.0001$, ns: not significant). The red line indicates the mean percentage of apoptosis. The error bars indicate the SEM.

Furthermore, we investigated whether synthetic cecropin A peptides injected into the *mxc* mutant larvae could also induce apoptosis in the LG tumors. As synthetic cecropin A of *H. cecropia* was commercially available, we injected the solutions into *mxc*^{mbn1} larvae at the third instar stage. Fifteen hours later, we observed whether the apoptosis areas in the mutant LGs increased compared to the areas of mutant larvae injected with PBS only (**Figure 6**a-d). The average percentage of the cDcp1-positive areas within the mutant LGs increased by 48.3%, compared with the PBS-injected control (**Figure 6**e). The difference was statistically significant ($p < 0.01$, **Figure 6**e). These results suggest that synthetic cecropin A peptides of a different species can also induce apoptosis in *Drosophila* LG tumors.

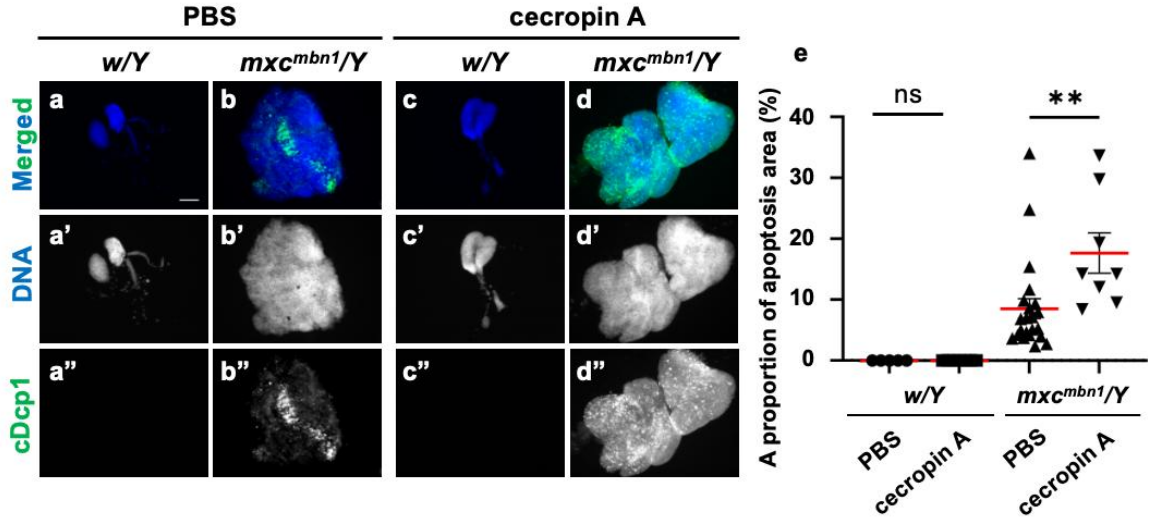

Figure 6. Apoptosis area quantification in *mxc*^{mbn1} larvae LGs after synthetic cecropin A peptide injection. . (**a**-**d**) Immunostaining of LGs in control (**a**, **c**) and *mxc*^{mbn1} (**b**, **d**) larvae with anti-cDcp1 antibodies that recognize apoptotic cells. Larvae at the third instar stage injected with PBS (control; **a**, **b**) or synthetic cecropin A (**c**, **d**) dissolved in PBS. Green (white in **a''**-**d''**) indicates a signal of anti-cDcp1 immunostaining, and blue (white in **a'**-**d'**) indicates DNA staining. Scale bars: 100 μm. (**e**) Quantification graphs indicate the percentage of apoptotic cells in the lobe regions of LGs after injecting PBS (n = 5 LGs from 3 *w/Y* and n = 22 LGs from 11 *mxc*^{mbn1}*/Y* larvae), and cecropin A (n = 7 LGs from 4 *w/Y* and n = 8 LGs from 4 *mxc*^{mbn1}*/Y* larvae). One-way ANOVA was used for multiple comparisons (**$p < 0.01$, ns: not significant). The red line indicates the mean percentage of apoptosis. The error bars indicate the SEM.

3.6. Dro or CecA1 overexpression in the fat body did not affect cell proliferation in the LGs of mxc^{mbn1} *larvae*

Presumably, another potential anti-tumor mechanism of these two AMPs may be the inhibition of LG cell proliferation. To test this possibility, we observed mitotic cells in the LGs of mutant larvae overexpressing *Dro* or *CecA1* in the fat body. Anti-phosphorylated histone H3 immunostaining revealed 3.0% (n = 20) mitotic cells of the total lobe region in normal LGs (**Figure S3**a-c). Although

 doi:10.20944/preprints202501.2343.v1

this percentage was approximately 30% higher than the average of 4.0% (n = 20) in *mxc*^{mbn1}*/Y; r4>+* (**Figure S3**d), the differences were not statistically significant. Next, we observed mitotic cells in 14.8% of the total lobe area in *Dro*-overexpressing third instar stage mutant larvae (*mxc*^{mbn1}*/Y; r4>Dro*) LG (**Figure S3**e). Although this percentage reduced from average (16.0%, n = 20) in LGs of *mxc*^{mbn1}*/Y; r4>+* (n = 20), the difference was not statistically significant (p = 0.347, **Figure S3**g). Thus, Drosocin overexpression failed to alter cell proliferation in the LG tumors of *mxc*^{mbn1} mutants.

Similarly, we induced *CecA1* overexpression in the fat body and performed anti-PH3 immunostaining of LGs in the larvae at the third instar stage using anti-PH3 antibody. Inducing *CecA1* expression in the fat body of *mxc*^{mbn1} mutant larvae (*mxc*^{mbn1}*/Y; r4>CecA1*) resulted in immunostaining of an average of 16.4% (n = 17) of the total lobe area in the LG of third instar stage larvae, similar to 16.0% in *mxc*^{mbn1}*/Y; r4>+* larvae (n = 20) (**Figure S3**d, f). However, this difference was not statistically significant (p = 0.44, **Figure S3**g). Thus, similar to Drosocin, Cecropin A overexpression did not affect cell proliferation in *mxc*^{mbn1} LG tumors.

3.7. Incorporation of Cecropin A into the circulating hemocytes in tumor-bearing mxc^{mbn1} *but not in control larvae*

Next, we investigated how Cecropin A, synthesized in the fat body and secreted into the hemolymph, acts on LG tumors (**Figure 7**). Other AMPs—Drosomycin, Diptericin, and Defensin—are incorporated into hemocytes in the hemolymph of tumor-bearing larvae in *mxc*^{mbn1}. We therefore investigated whether Cecropin A has a similar property. HA-tagged Cecropin A was expressed in the fat body of *mxc*^{mbn1} larvae (*mxc*^{mbn1}*/Y; r4 > CecA1-HA*) and immunostaining of the circulating hemocytes was performed with anti-HA antibody to see whether it would be taken up by the cells. We observed HA immunostaining signals indicating Cecropin A inside 59.5% of hemocytes in the *mxc* mutant larvae (n = 450 hemocytes from 7 larvae were examined) (**Figure 7**b″). In contrast, we found few signals in the hemocytes of control larvae (n = 443 cells from 10 larvae)(**Figure 7**a″).

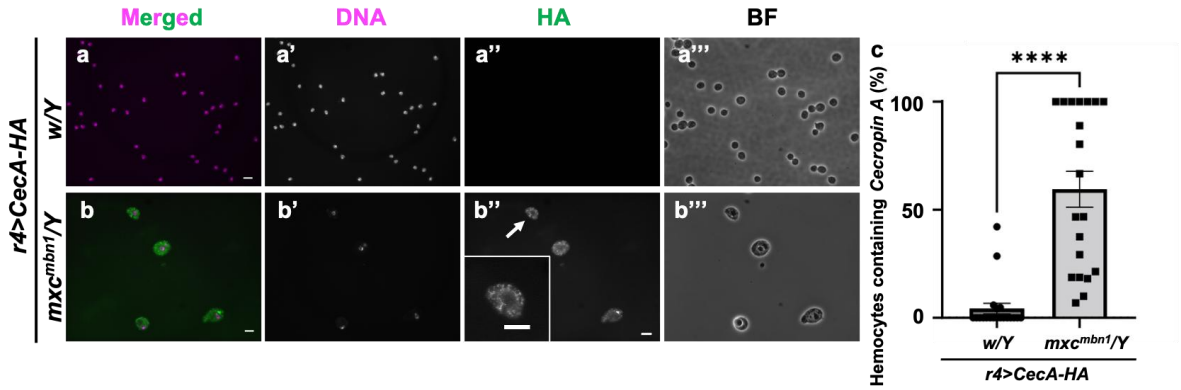

Figure 7. Observation of circulating hemocytes in which HA-tagged Cecropin A produced in the fat body was incorporated in control and *mxc*^{mbn1} larvae. (**a**, **b**) Anti-HA immunostaining of circulating hemocytes in normal (*w/Y; r4>CecA1-HA*) (**a**) and *mxc*^{mbn1} larvae (*mxc*^{mbn1}*/Y; r4>CecA1-HA*) (**b**) expressing Cecropin A-HA in the fat body. Green, fluorescence of anti-HA immunostaining (white in **a″**, **b″**); magenta, DNA (white in **a′**, **b′**). A magnified image of the hemocyte pointed by an arrow is presented in the insets in b″. Scale bars: 10 μm. (**c**) Percentages of the hemocytes harboring HA-tagged Cecropin A in control and *mxc*^{mbn1} larvae. Significant differences were determined using Welch's t test (****p < 0.0001, n = 20). The error bars indicate SEM.

3.8. Drosomycin incorporation into the hemocytes required Draper signaling in mxc^{mbn1} *larvae*

Next, we investigated the specific mechanism by which AMPs known to possess anti-tumor properties are taken up into the circulating hemocytes in the *mxc* mutant larvae bearing the LG tumor. As we speculated that endocytosis factors mediate the process, we depleted mRNA for Draper, a phagocytosis factor, specifically in the hemocytes. Since antibodies against Cecropin A or other well-

 doi:10.20944/preprints202501.2343.v1

known AMPs are unavailable, we used the stock that permits the expression of GFP-tagged Drosomycin under its gene promoter (*Drs::GFP*). This AMP is also incorporated into the circulating hemocytes in the mutant larvae [26]. We examined the cellular localization of the anti-tumor AMP in the hemocytes using this GFP fusion protein. GFP signals indicative of Drosomycin were not detected in the hemocytes of *w, Drs::GFP/Y* larvae (374 hemocytes from 6 larvae, 30 fields on the microscope) (**Figure 8**a″). By contrast, a 10-fold increase in fluorescence intensity was detected in the cytoplasm of hemocytes in *mxc*^{mbn1}, *Drs::GFP/Y* larvae (1,021 cells from 8 larvae, 40 fields on the microscope) (**Figure 8**b″). There were no alterations in the number of circulating hemocytes in larvae harboring hemocyte-specific depletion of phagocytosis factors, Draper and Shark (*w/Y; He > drprRNAi* and *w/Y; He > sharkRNAi*) compared to control larvae (*w/Y*), suggesting that depletion of these factors did not affect hemocyte survival. Thus, we next depleted these mRNAs specifically in the hemocytes of the mutant larvae (**Figure 8c, d**). The number of GFP^{+} cells decreased to 5.1% and 3.5 % (107 cells/2,098 cells, 40 fields, and 42 cells/1,193 cells, 30 fields, respectively) compared to 39.5% (360 cells/1,021 cells, 40 fields) of hemocytes the depletion (*mxc*^{mbn1}, *Drs::GFP; He>+*). The differences are significant in both cases ($p < 0.0001$) (**Figure 8**e). The intensities of the GFP signal indicative of Drosomycin within the hemocytes also decreased below a background level (**Figure 8**b″-d″). From these results, we concluded that when *drpr* or *shark* mRNA is depleted in hemocytes, the uptake of *Drs* is inhibited. In other words, this suggests that the Draper signaling in hemocytes is indispensable for the uptake of into hemocytes in *mxc*^{mbn1} larvae.

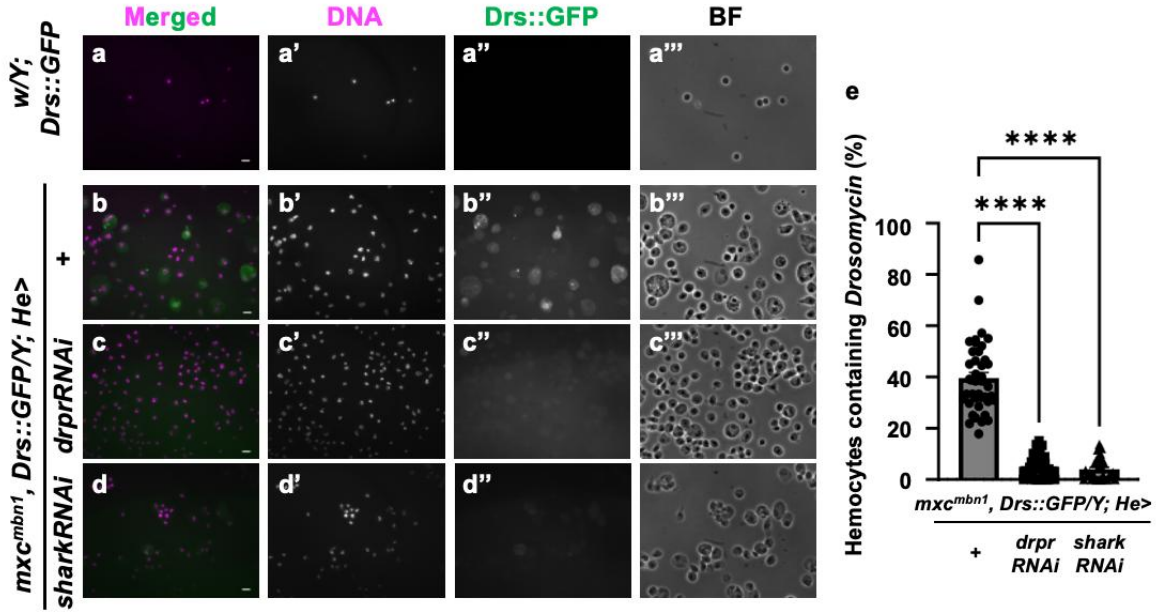

Figure 8. Observation and quantification of hemocytes in which GFP-tagged Drosomycin was incorporated in control and *mxc*^{mbn1} larvae. (**a**, **b**) GFP fluorescence of circulating hemocytes to detect GFP-tagged Drosomycin (a, b), induced in the FB of control (*w, Drs::GFP/Y*)(**a**) and *mxc*^{mbn1} (*mxc*^{mbn1}, *Drs::GFP/Y*) (**b**) larvae. (**c**, **d**) GFP fluorescence indicating GFP-tagged Drosomycin in the circulating hemocytes of the mutant larvae harboring hemocyte-specific knockdown of *draper* (*mxc*^{mbn1}, *Drs::GFP/Y; He>drprRNAi*) (**c**), or *shark* (*mxc*^{mbn1}, *Drs::GFP/Y; He>sharkRNAi*) (**d**). The circulating hemocytes harboring GFP-tagged Drosomycin (Drs::GFP) are colored in green in **a**-**d** (white in (**a″**-**d″**). DNA is magenta in **a**-**d** (white in **a′**-**d′**). Scale bars: 10 μm. (**e**) Percentages of the hemocytes harboring GFP-tagged Drosomycin in control and *mxc*^{mbn1} larvae. X-axis from left to right: control larvae expressing GFP-tagged Drosomycin under its promoter (*w, Drs::GFP/Y* (n = 374 hemocytes (6 larvae)), *mxc*^{mbn1}, *Drs::GFP/Y* (n = 1,021 (8)), *mxc*^{mbn1}, *Drs::GFP/Y; He>drprRNAi* (n = 2,098 (8)), and *mxc*^{mbn1}, *Drs::GFP/Y; He>sharkRNAi* (n = 1,193 (6)) larvae. One-way ANOVA was used for multiple comparisons (****$p < 0.0001$). The error bars indicate SEM.

 doi:10.20944/preprints202501.2343.v1

Furthermore, to exclude the possibility that gene transcription was induced in the *mxc* mutant hemocytes, we monitored its gene expression using a *Drs-YFP* reporter. We did not see any YFP signals indicating its expression in the *mxc*^{mbn1} mutants and the controls (**Figure S4**a', b', n = 245 hemocytes from 5 larvae). From these results, we concluded that *Drs* is not transcribed in circulating hemocytes in the *mxc*^{mbn1} mutant larvae. Based on these results, Drosomycin is incorporated, but not transcribed, into circulating hemocytes, specifically those of the *mxc*^{mbn1} larvae bearing the LG tumors, which require phagocytosis factors: Draper and Shark.

3.9. Phosphatidylserine localization on the plasma membrane surface in LG tumors

Phosphatidylserine (PS) is exposed on the lipid bilayer surface in cancer cells and serves as a marker for phagocytosis by macrophages. In the lipid bilayers of tumors arising on the wing discs in *Drosophila dlg* mutants, more PS is exposed on the surface than in the wild type [29]. Therefore, we hypothesized PS localization on the cell surface in LG tumors of *mxc*^{mbn1} mutants. To test this, we induced ectopic expression of Annexin V-GFP, which has a strong affinity for PS, in the fat body to allow hemolymph secretion. We observed GFP fluorescence in the LG tumors of *mxc*^{mbn1} larvae (*mxc*^{mbn1}*/Y; r4>Annexin V-GFP*) but not in normal controls (*w/Y; r4>Annexin V-GFP*) (**Figure 9**a'', b''), indicating Annexin V binding. To quantify the percentage of GFP signal regions in the LG lobe regions, fixed LG samples were stained with DAPI, and the surface area of the entire LG lobe region was measured. The Annexin V-binding region (mean: 26.8%) (n = 16) increased in the LG of *mxc*^{mbn1} mutants compared to that in normal controls (n = 20) (**Figure 9**c) ($p < 0.0001$). Thus, we concluded that PS was exposed on the cell membrane surface in *mxc*^{mbn1} LG tumors.

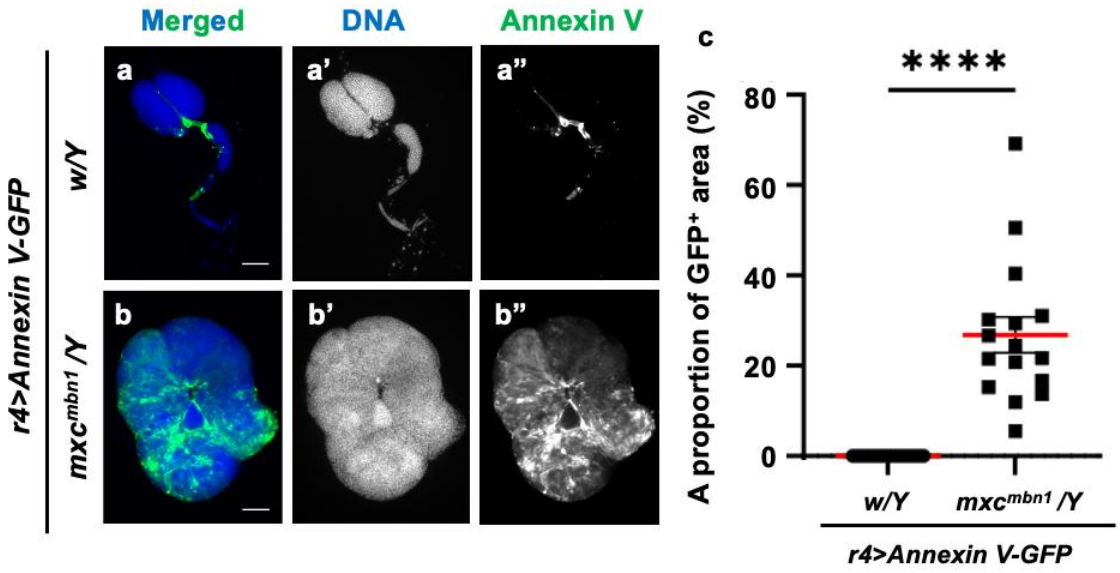

Figure 9. Detection of phosphatidylserine (PS) exposed on the cell surface of lymph gland (LG) tumors from control and *mxc*^{mbn1} larvae. (**a**, **b**) DAPI-stained fluorescence images of LGs from larvae at the third instar stage: (**a**) normal control, (**b**) *mxc*^{mbn1} mutant. Blue indicates DNA staining and green indicates Annexin V-GFP signal. Scale bars: 100 μm. (**c**) Quantification graph indicating the percentage of GFP fluorescent regions in LGs, indicative of Annexin V binding. Significant differences were determined using Welch's *t* test (****$p < 0.0001$, n = 16). The red line indicates the mean percentage. The error bars indicate SEM.

3.10. Xkr scramblase knockdown canceled PS localization on the surface of LG cells and led to LG hyperplasia enhancement in mxc^{mbn1}

To confirm whether PS is indeed used as a target of tumor suppression, we depleted the mRNA for scramblase required to expose PS to the cell surface and examined its effect on LG tumor growth.

 doi:10.20944/preprints202501.2343.v1

For this purpose, we induced double-stranded RNAs against *xkr scramblase* mRNA using the known *UAS-xkrRNAi* stock [52] and the *upd3-Gal4* driver, in which Gal4 is expressed in the undifferentiated cell region of the LG: the origin from which the LG tumors arise [37]. The fluorescence indicating Alexa594-Annexin V binding almost disappeared from the *xkrRNAi* LGs, as shown in **Figure 10**c''. In other words, the PS signal exposed to the cell surface in the LG tumor region was reduced. In these larvae, the LG tumor size increased to an average of approximately twice that of the control (**Figure 10**d). This difference was statistically significant ($p < 0.05$). Based on these results, we conclude that PS exposure on the surface of tumor cells is required to target anti-tumor proteins, such as Drosomycin to the LG tumor.

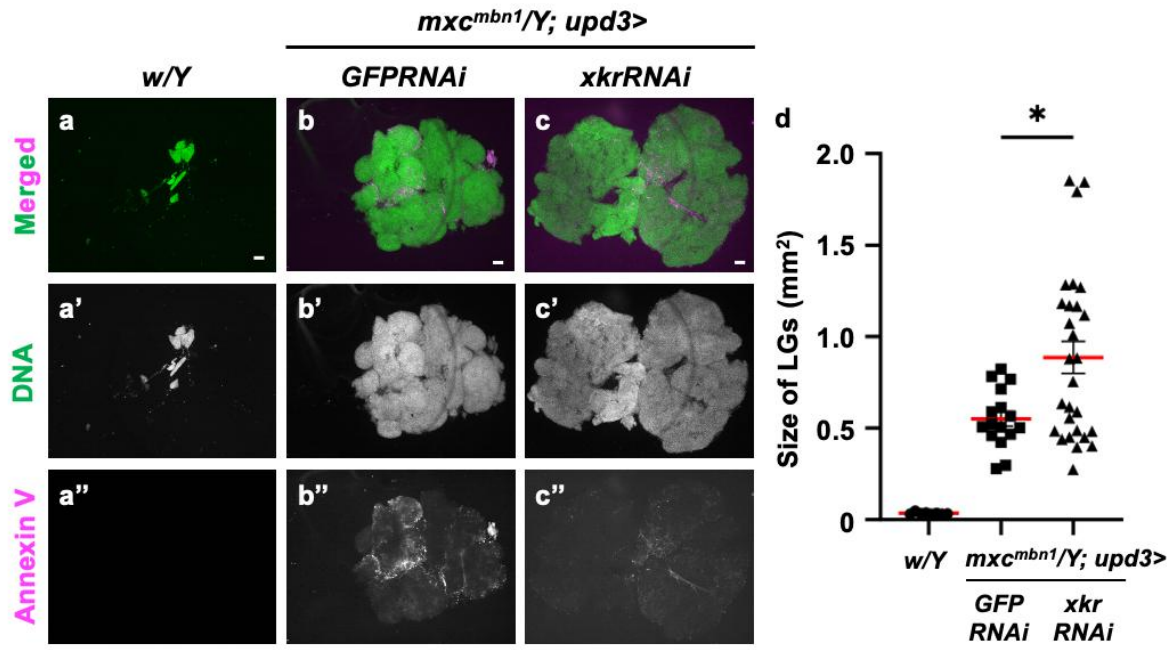

Figure 10. Loss of PS on the surface of LG cells by Xkr scramblase knockdown and its influence on LG hyperplasia in *mxc*^{mbn1} larvae. (**a**-**c**) DAPI-stained anterior lobes and fluorescence indicating Alexa 594-Annexin V binding to PS on the LG lobes in normal controls (*w*/*Y*) (**a**), *mxc*^{mbn1} with ectopic expression of control dsRNA in the medulla zone in primary lobes of the LG (*mxc*^{mbn1}*/Y; upd3>GFPRNAi*) (**b**), and *mxc*^{mbn1} with depletion of *xkr* mRNA (*mxc*^{mbn1}*/Y; upd3>xkrRNAi*) (**c**) in the larvae at the third instar stage. DNA is stained in blue in **a**-**c** (white in **a'**-**c'**), and Alexa594-Annexin-V is in magenta in **a**-**c** (white in **a''**-**c''**). Scale bars: 100 μm. (**d**) Quantification of the LG size of *mxc*^{mbn1} harboring *xkr* depletion in the LG tumor cells. The average LG size was calculated among the controls (*w*/*Y*) (n = 9 LGs (5 larvae)), *mxc*^{mbn1}*/Y; upd3>GFPRNAi* (n = 16 (8)), and *mxc*^{mbn1}*/Y; upd3>xkrRNAi* (n = 28 (14)). One-way ANOVA multiple comparisons (*$p < 0.05$). The red line indicates the mean percentage of apoptosis. The red line indicates the mean LG size. The error bars indicate the SEM.

4. Discussion

4.1. Cecropin A and Drosocin induction via the innate immune pathways in the fat body of mxc^{mbn1} *mutant larvae bearing the LG tumors*

This study demonstrated that the levels of mRNAs encoding Cecropin A and Drosocin were elevated in the fat body of *mxc*^{mbn1} larvae bearing LG tumors. This upregulation depended on both the Toll-and Imd-mediated immune pathways. These findings suggest that the innate immune system plays a role in suppressing cancer cells, even in *Drosophila*. In mammals, both the innate and acquired immune systems are involved in eliminating cancer cells [53,54,55,56]. By contrast, invertebrates lack an acquired immune system. Consequently, the tumor-suppressive effects described in this study are attributable to the innate immune system. This process involves the

 doi:10.20944/preprints202501.2343.v1

participation of plasmatocytes, which are macrophage-like cells in *Drosophila* hemolymph [32,36]. In *mxc*^{mbn1} larvae with LG tumors, circulating hemocytes can recognize damage to the basement membrane and subsequently accumulate on the tumors [35]. Additionally, as this LG tumor expresses Eiger/a tumor necrosis factor (TNF) orthologue, the hemocytes recognize it via Eiger receptors on the cell surface, thereby inducing Turandot family proteins with anticancer effects [32]. Therefore, in *Drosophila*, cells of the innate immune system can recognize the tumor and transmit this information to the fat body. The induction of Cecropin A and Drosocin is interpreted as induced via a similar inter-tissue communication. Furthermore, crosstalk between the fat body and hemocytes is also needed to suppress tumors that arise in the wing imaginal discs. In this instance, active Spätzle, generated by the reactive oxygen species accumulated in hemocytes, activates Toll in the fat body cells [28,35]. In contrast, the mechanism by which the Imd pathway is activated in response to tumors remains unelucidated. The present study demonstrates that the induction of Cecropin A and Drosocin in the fat body is diminished in *mxc*^{mbn1} mutants when the doses of the genes for signaling factors in the Imd pathway are halved. The expression of these two AMPs during bacterial infection is regulated by both the Toll and Imd pathways [9]. It was reported that these two pathways engage in cross-talk [57]. Consequently, a Toll-mediated signal is triggered by Spätzle around tumor-responsive hemocytes associated with the fat body. This may also activate the Imd pathway, eventually inducing target AMP gene expression.

4.2. Cytotoxic effects of Cecropin A and Drosocin on tumors in Drosophila larvae

This study showed that Cecropin A and Drosocin overexpression in the fat body increased apoptosis induction and consequently reduced LG tumor size in *mxc*^{mbn1} larvae. Therefore, we conclude that these two AMPs have anti-tumor effects against LG tumors of *mxc*^{mbn1} larvae. These results are consistent with the previous findings that five other AMPs—Drosomycin, Diptericin, Defensin, Metchinikowin, and Attacin A—and two Turandot family proteins—TotB and TotF—possess antitumor properties that suppress tumor growth in *Drosophila* [26,29,58]. Moreover, this study demonstrated that synthetic cecropin A peptides of Cecropia moth can also stimulate apoptosis in the LG tumor in *Drosophila*. Consistently, housefly cecropin also induces apoptosis in human hepatocellular carcinoma cells without affecting normal cells [59]. Synthetic cecropin A possesses anticancer properties against leukemia cell lines [60,61]. These studies were performed to check the anticancer properties of AMPs of other species *in vitro*. By contrast, we demonstrated that cecropin A stimulated apoptosis in tumors in living organisms. Our experimental system may be used as a simple *in vivo* model to determine if the anti-cancer drug candidates stimulate apoptosis and suppress tumor growth. Cecropin B also exhibits selective antitumor activity against human cancer cells, which can be applied to anticancer cell therapy [62,63]. Therefore, cecropin B may exhibit a stronger antitumor effect. This will be investigated in our future study.

4.3. Tumor-specific effect of Cecropin A and Drosocin on LG tumors in mxc^{mbn1} *larvae may be determined by the circulating hemocytes that take up AMPs*

The detailed mechanism of the cytotoxic effects of AMPs on tumors while sparing normal cells remains unclear [63,64]. Drosomycin, Defensin, and Turandots are taken up by the circulating hemocytes in the *mxc*^{mbn1} mutant larvae bearing tumors but not normal larvae [26,32,58]. Basement membrane damage in LG tumors is involved in tumor cell recognition by circulating hemocytes, resulting in their accumulation [35]. Eiger, a *Drosophila* TNF orthologue, is ectopically expressed in the LG tumors of *mxc*^{mbn1} larvae. When hemocytes receive it via the Eiger receptor on the cell surface, Upd3—a *Drosophila* functional IL-6 orthologue—is induced. This is essential in transmitting information to the fat body [32]. Circulating hemocytes that recognize LG tumors may take up the AMPs in this way and accumulate in LG tumors again. The AMPs are then released from the hemocytes and can act locally on tumors.

This study demonstrated that the circulating hemocytes of *mxc*^{mbn1} larvae take up Cecropin A, although the mechanism remains unclear. The localization of HA-tagged AMP specifically induced

 doi:10.20944/preprints202501.2343.v1

using a fat-body specific Gal4 driver was investigated employing anti-HA immunostaining. Knocking down the genes required for hemocyte uptake using another driver in the same larvae is challenging. Antibodies to detect either AMP were unavailable, despite our efforts to generate them. We will continue to raise them and investigate the localization of Drosocin. Instead, we investigated the uptake of Drosomycin using the strain in which the GFP-tagged peptides can be induced under its promoter. We observed GFP fluorescence in the hemocytes of *mxc*^{mbn1} mutants but not in normal larvae, even though the gene was not transcribed in the hemocytes of the mutant larvae. This is consistent with the results that HA-tagged Drosomycin and other AMPs, including Cecropin A, are incorporated into the circulating hemocytes of the mutant larvae [26, this study]. Using the stock expressing GFP-tagged Drosomycin, we demonstrated that phagocytosis factors, Draper and Shark [65], are required for hemocyte uptake of the AMP. The AMP is possibly taken up into vacuoles, such as phagosomes, formed during phagocytosis. Previous studies described that Drosomycin is enclosed in cytoplasmic vesicles and is transported to the endosome system when it is released from the fat body into the hemolymph against bacterial infection [66,67]. Consistently, in response to tumor cells, these incorporated AMPs are likely transported to the plasma membrane via a recycling endosome pathway [68]. Subsequently, they may be released from the cells via exocytosis [69]. This hypothesis needs to be validated in the future .

4.4. Restrictive anti-cancer effects of AMPs on the LG tumor cells in which PS was exposed on the plasma membrane surface

This study showed that Cecropin A or Drosocin overexpression in the fat body of *mxc*^{mbn1} larvae stimulated apoptosis and suppressed LG tumor growth. Furthermore, the absence of apoptosis induction in tissues of normal larvae overexpressing Drosocin or Cecropin A suggested that these AMPs act in a strict tumor-specific manner. The cell membrane surface of normal cells is positively charged, whereas that of malignant tumor cells is negatively charged. This is due to the superficial presence of PS on the external plasma membrane surface [70]. PS is retained in the inner leaflet of the plasma membrane in normal cells by scramblase [71]. In cancer cells, however, PS is exposed on the cell surface because of reduced scramblase activity [72]. The relationship between PS density on the surface and cell sensitivity to AMP has been suspected in several cancer cell lines, suggesting that PS plays a critical role in anti-cancer activity [73]. The negative surface charge of cancer cell membranes is shared by bacterial cells [64,74]. Thus, AMPs may attack tumors through a mechanism similar to that of bacteria. This implies that AMPs with positively charged amino acid sequences may easily bind to negatively charged cancer cell membranes. On insertion in the cell membrane, they can kill cancer cells by rupturing the membrane [75]. PS is prevalent on the surface of the plasma membrane in *Drosophila* wing disc tumors and Defensin acts by marking this PS on the surface of the tumors [29]. This study observed that Annexin V, which acts through the hemolymph, binds to the cell surface in LG tumors, sparing healthy tissues. Thus, conceivably, PS is similarly exposed on the surface of *Drosophila* LG tumor cells of *mxc*^{mbn1} larvae, which may facilitate AMPs' tumor cell targeting. Thus, AMPs act on PS as a landmark, resulting in apoptosis. Taken together, we can speculate the following story: when hemocytes recognize LG tumors, they take up AMPs via phagocytosis and are recruited very close to the LG tumor, where AMPs are released. In addition to the role of hemocytes in the limitation of AMPs' action range, their possible target, tumor cell surface PS, further restricts AMPs' antitumor effect. Notably, an important factor in developing anti-cancer drugs is the absence of side effects. If the tumor-specific anti-cancer effects of the AMPs are proven and their acting mechanism elucidated, they are expected to constitute anti-cancer drugs with minimal side effects.

Finally, we discuss the study limitations and several issues to be addressed in the future. First, Cecropin A is incorporated into hemocytes in larvae with tumors, while Drosocin uptake has not been investigated. Antibodies that can be used for immunostaining have not been obtained. This is a limitation of this study. In future studies, we would establish a UAS line that expresses HA-tagged Drosocin and confirm its tumor-dependent uptake. Second, although we found that synthetic

 doi:10.20944/preprints202501.2343.v1

AMP peptides of insects other than *Drosophila* can also induce apoptosis in the mxc^{mbn1} tumors, many AMPs are not conserved between species. Exceptionally, some defensin family members are also conserved in mammals [76]. Another issue is investigating mammalian synthetic defensins' effects on LG tumors. Some AMPs require post-translational modifications such as glycosylation for their cytotoxic effects. If so, these effects may not be observed in synthetic peptides. This is a problem with this method. While the effects cannot be studied as readily as synthetic peptides, it is possible to determine whether it can suppress tumor growth by expressing mammalian AMPs in *Drosophila*. Third, we have shown that Drosomycin uptake requires phagocytosis factors, Draper and Shark; however, how AMPs are taken into the cell remains to be elucidated. Previous studies suggest that they are inserted into the plasma membrane and that the cellular membrane is subsequently disrupted. When such peptides are enclosed in the phagosome, the reason why they do not act on the isolating membrane is not understood. The mechanism by which the enclosed AMPs are secreted outside the hemocytes must also be identified. Exocytosis is presumed to be involved, but it is necessary to verify this through knockdown experiments of the genes required.

5. Conclusions

Two major AMPs in *Drosophila*, Cecropin A and Drosocin, are induced in the *mxc* mutant larvae harboring the LG tumors depending on the innate immune pathway. These AMPs specifically exert cytotoxic effects on the tumors by enhancing apoptosis. The AMPs synthesized in the fat body are incorporated into the macrophage-like blood cells in the mutant, not in normal larvae. Another AMP, Drosomycin, is incorporated via the Draper-mediated phagocytotic signaling. After being transported to the vicinity of the tumors, the AMPs released from the blood cells may target phosphatidylserine exposed on the tumor surface for apoptosis induction. Synthetic cecropin A peptides of another organism also showed an apoptosis-inducing property. They are expected to be anti-cancer drugs with minimal side effects.

Supplementary Materials: The following supporting information can be downloaded at: www.mdpi.com/xxx/s1, Figure S1: The mRNA levels of *Dro* and *CecA* genes in the fat body and LG tumor size of mxc^{mbn1} larvae heterozygous for mutations of the genes encoding the factors in innate immune pathways. Figure S2: Immunostaining and quantification of apoptosis in wing imaginal discs of control larvae harboring fat body-specific induction of *Dro* or *CecA1* overexpression. Figure S3: Immunostaining and quantifying cell proliferation in LGs of mxc^{mbn1} larvae with a fat body-specific expression of *Dro* or *CecA1*. Figure S4: Absence of the *Drs* gene transcription in hemocytes, as confirmed by the *Drs-YFP* reporter in mxc^{mbn1} larvae.

Author Contributions: Conceptualization, Y.H.I.; methodology, M.H. and Y.HI.; validation, M.H., and Y.H.I.; formal analysis, M.H.; investigation, M.H.; resources, Y.H.I.; data curation, Y.H.I.; writing—original draft preparation, M.H.; writing—review and editing, Y.H.I.; visualization, X.X.; supervision, Y.H.I and T.N.; project administration, Y.H.I.; funding acquisition, Y.H.I. All authors have read and agreed to the published version of the manuscript.

Funding: This study was partially supported by Grant-in-Aid for Scientific Research C (17K07500) to YHI.

Institutional Review Board Statement: The animal study protocol was approved by the Kyoto Institute of Technology Review Board (protocol code: R4-11 and date of approval: 24 January 2023).

Data Availability Statement: The datasets generated and/or analyzed in the current study are available from the corresponding author upon reasonable request.

Acknowledgments: This study was partially supported by Grant-in-Aid for Scientific Research C (17K07500) to YHI. We are grateful to BDSC, VDRC, B. Lemaitre (École Polytechnique Fédérale de Lausanne, Swiss), C. Han (Cornell University, NY, USA), M. Miura (University of Tokyo, Tokyo, Japan), Y. Yagi (Nagoya University, Nagoya, Japan) for providing fly stocks or antibodies.

Conflicts of Interest: The authors declare no conflicts of interest.

 doi:10.20944/preprints202501.2343.v1

References

1. Lemaitre, B.; Hoffmann, J. The host defense of *Drosophila melanogaster*. *Annu. Rev. Immunol.* **2007**, *25*, 697–743.
2. Clark, R.; Kupper, T. Old meets new: The interaction between innate and adaptive immunity. *J. Invest. Dermatol.* **2005**, *125*, 629–637.
3. Willermain, F.; Rosenbaum, J.T.; Bodaghi, B.; Rosenzweig, H. L.; Childers, S.; Behrend, T.; Wildner, G.; Dick, A. D. Interplay between innate and adaptive immunity in the development of non-infectious uveitis. *Prog. Retin. Eye. Res.* **2012**, *31*, 182–194.
4. Nicolas, E.; Reichhart, J. M.; Hoffmann, J. A.; Lemaitre, B. In vivo regulation of the IκB homologue Cactus during the immune response of *Drosophila*. *J. Biol. Chem.* **1998**, *273*, 10463–10469.
5. Brennan, A.; Anderson, V. *Drosophila*: the genetics of innate immune recognition and response. *Annu. Rev. Immunol.* **2004,** *22*, 457–483.
6. Hoffmann, J.A. The immune response of *Drosophila*. *Nature* **2003**, *426*, 33–38.
7. Leclerc, V., and Reichhart, J.-M. The immune response of *Drosophila* melanogaster. *Immunol. Rev.* **2004**, *198*, 59–71.
8. Hoffmann, J.A.; Reichhart, J.-M. *Drosophila* innate immunity: an evolutionary perspective. *Nat. Immunol.* **2002**, *3*, 121–126.
9. Tzou, P.; Reichhart, J.-M.; Lemaitre, B. Constitutive expression of a single antimicrobial peptide can restore wild-type resistance to infection in immunodeficient *Drosophila* mutants. *Proc. Natl. Acad. Sci. USA.* **2002**, *99*, 2152–2157.
10. Lemaitre, B.; Reichhart, J.-M.; Hoffmann, J. A. *Drosophila* host defense: Differential induction of antimicrobial peptide genes after infection by various classes of microorganisms. *Proc. Natl. Acad. Sci. U.S.A.* **1997**, *94*, 14614–14619.
11. Lindsay, S. A.; Wasserman, S. A. Conventional and non-conventional *Drosophila* Toll signaling. *Dev. Comp. Immunol.* **2014**, *42*, 16–24.
12. Gobert, V.; Gottar, M.; Matskevich, A. A.; Rutschmann, S.; Royet, J.; Belvin, M.; Hoffmann, J. A.; Ferrandon, D. Dual activation of the *Drosophila* Toll pathway by two pattern recognition receptors. *Science* **2003**, *302*, 2126–2130.
13. Gottar, M.; Gobert, V.; Matskevich, A. A.; Reichhart, J.-M.; Wang, C.; Butt, T. M.; Belvin, M.; Hoffmann, J. A.; Ferrandon, D. Dual detection of fungal infections in *Drosophila* via recognition of glucans and sensing of virulence factors. *Cell* **2006**, *127*, 1425–1437.
14. Valanne, S.; Wang, J.-H.; Rämet, M. The *Drosophila* Toll signaling pathway. *J. Immunol.* **2011**, *186*, 649–656.
15. Sun, H.; Bristow, B.N.; Qu, G.; Wasserman, S.A. A heterotrimeric death domain complex in Toll signaling. *Proc. Natl. Acad. Sci. U.S.A.* **2002** *99*, 12871–12876.
16. Gottar, M.; Gobert, V.; Michel, T.; Belvin, M.; Duyk, G.; Hoffmann, J. A.; Ferrandon, D.; Royet, J. The *Drosophila* immune response against Gram-negative bacteria is mediated by a peptidoglycan recognition protein. *Nature* **2002**, *416*, 640–644.
17. Kleino, A.; Silverman, N. The *Drosophila* IMD pathway in the activation of the humoral immune response. *Dev. Comp. Immunol.* **2014**, *42*, 25–35.
18. Buchon, N.; Silverman, N.; Cherry, S. Immunity in *Drosophila* melanogaster — from microbial recognition to whole-organism physiology. *Nat. Rev. Immunol.* **2014**, *14*, 796–810.
19. Ertürk-Hasdemir, D.; Broemer, M.; Leulier, F.; Lane, W. S.; Paquette, N.; Hwang, D.; Kim, C.-H.;

 doi:10.20944/preprints202501.2343.v1

Stöven, S.; Meier, P.; Silverman, N. Two roles for the *Drosophila* IKK complex in the activation of Relish and the induction of antimicrobial peptide genes. *Proc. Natl. Acad. Sci. U.S.A.* **2009**, *106*, 9779–9784.

20. Kleino, A.; Silverman, N. The *Drosophila* IMD pathway in the activation of the humoral immune response. *Dev. Comp. Immunol.* **2014**, *42*, 25–35.
21. Tanji, T.; Ip, Y. T. Regulators of the Toll and Imd pathways in the *Drosophila* innate immune response. *Trends Immunol.* **2005**, *26*, 193–198.
22. Hultmark, D.; Steiner, H.; Rasmuson, T.; Boman, H. G. Insect immunity. purification and properties of three inducible bactericidal proteins from hemolymph of immunized pupae of *Hyalophora cecropia*. *Eur. J. Biochem.* **1980**, *106*, 7–16.
23. Chen, H.M.; Wang, W.; Smith, D.; Chan, S.C. Effects of the anti-bacterial peptide cecropin B and its analogs, cecropins B-1 and B-2, on liposomes, bacteria, and cancer cells. *Biochim Biophys Acta.* **1997**, *1336*, 171–179.
24. Chan, S.C.; Hui, L.; Chen, H.M. Enhancement of the cytolytic effect of anti-bacterial cecropin by the microvilli of cancer cells. *Anticancer Res.* **1998**, *18*, 4467–474.
25. Moore, A.J.; Devine, D.A.; Bibby, M.C. Preliminary experimental anticancer activity of cecropins. *Pept. Res*. **1994**, *7*, 265–269.
26. Araki, M.; Kurihara, M.; Kinoshita, S.; Awane, R.; Sato, T.; Ohkawa, Y.; Inoue, Y.H. Anti-tumour effects of antimicrobial peptides, components of the innate immune system, against hematopoietic tumors in *Drosophila mxc* mutants. *Dis. Model. Mech.* **2019**, *12*, dmm037721.
27. Arefin, B.; Kunc, M.; Krautz, R.; Theopold, U. The immune phenotype of three *Drosophila* leukemia models. *G3: Genes Genomes Genet.* **2017**, *7*, 2139–2149.
28. Parisi, F.; Stefanatos, R. K.; Strathdee, K.; Yu, Y.; Vidal, M. Transformed epithelia trigger non-tissue-autonomous tumor suppressor response by adipocytes via activation of Toll and Eiger/TNF signaling. *Cell Rep.* **2014**, *6*, 855–867.
29. Parvy, J.-P.; Yu, Y.; Dostalova, A.; Kondo, S.; Kurjan, A.; Bulet, P.; Lemaître, B.; Vidal, M.; Cordero, J. B. The antimicrobial peptide Defensin cooperates with Tumour Necrosis Factor to drive tumor cell death in *Drosophila*. *eLife* **2019**, *8*, e45061.
30. Lebestky, T.; Chang, T.; Hartenstein, V.; Banerjee, U. Specification of *Drosophila* hematopoietic lineage by conserved transcription factors. *Science* **2000**, *288*, 146–149.
31. Sanche Bosch, P.; Makhijani, K.; Herboso, L.; Gold, KS.; Baginsky, R.; Woodcock, KJ.; Alexander, B.; Kukar, K.; Corcoran, S.; Jacobs, T.; Ouyang, D.; Wong, C.; Ramond, EJV.; Rhiner, C.; Moreno, E.; Lemaitre, B.; Geissmann, F.; Brückner, K. Adult *Drosophila* lack hematopoiesis but rely on a blood cell reservoir at the respiratory epithelia to relay infection signals to surrounding tissues. *Dev. Cell* **2019**, *51*, 787–803.
32. Kinoshita, J.; Kinoshita, Y.; Nomura, T.; Inoue, Y.H. Macrophage-like blood cells are involved in inter-tissue communication to activate JAK/STAT signaling, inducing antitumor Turandot proteins in *Drosophila* fat body via the TNF-JNK pathway. *Int. J. Mol. Sci.* **2024**, *25*, 13110.
33. Hanahan, D.; Weinberg, R. A. Hallmarks of cancer: the next generation. *Cell* **2011**, *144*, 646–674.
34. Cordero, J. B.; Macagno, J. P.; Stefanatos, R. K.; Strathdee, K. E.; Cagan, R. L.; Vidal, M. Oncogenic Ras diverts a host TNF tumor suppressor activity into tumor promoter. *Dev. Cell* **2010**, *18*, 999–1011.
35. Kinoshita, S.; Takarada, K.; Kinoshita, Y.; Inoue, Y. H. *Drosophila* hemocytes recognize lymph gland tumors of *mxc* mutants and activate the innate immune pathway in a reactive oxygen species-dependent manner. *Biol. Open* **2022**, *11*, bio059523.

 doi:10.20944/preprints202501.2343.v1

36. Pastor-Pareja, J. C.; Wu, M.; Xu, T. An innate immune response of blood cells to tumors and tissue damage in *Drosophila*. *Dis. Model. Mech.* **2008**, *1*, 144–154.
37. Kurihara, M.; Komatsu, K.; Awane, R.; Inoue, Y. H. Loss of histone locus bodies in the mature hemocytes of larval lymph gland result in hyperplasia of the tissue in *mxc* mutants of *Drosophila*. *Int. J. Mol. Sci.* **2020**, *21*, 1586.
38. Remillieux-Leschelle, N., Santamaria, P., and Randsholt, N.B. Regulation of larval hematopoiesis in *Drosophila melanogaster*: a role for the *multi sex combs* gene. *Genetics* **2002**, *162*, 1259–1274.
39. Takarada, K.; Kinoshita, J.; Inoue, Y. H. Ectopic expression of matrix metalloproteinases and filopodia extension via JNK activation are involved in the invasion of blood tumor cells in *Drosophila mxc* mutant. *Genes. Cells.* **2023**, *28*, 709–726.
40. Tzou, P.; Ohresser, S.; Ferrandon, D.; Capovilla, M.; Reichhart, J.-M.; Lemaitre, B.; Hoffmann, J.A.; Imler, J.-L. Tissue-specific inducible expression of antimicrobial peptide genes in *Drosophila* surface epithelia. *Immunity* **2000**, *13*, 737–748.
41. Yagi, Y.; Lim, Y-M.; Tsuda, L.; Nishida, Y. fat facets induce polyubiquitination of Imd and inhibits the innate immune response in *Drosophila*. *Genes Cells*. **2013**, *18*, 934–945.
42. Schnorrer, F.; Schönbauer, C.; Langer, C.C.; Dietzl, G.; Novatchkova, M.; Schernhuber, K.; Fellner, M.; Azaryan, A.; Radolf, M.; Stark, A.; Keleman, K.; Dickson, B.J. Systematic genetic analysis of muscle morphogenesis and function in *Drosophila*. *Nature*. **2010**. *464*, 287–291.
43. Kira, A.; Tatsutomi, I.; Saito, K.; Murata, M.; Hattori, I.; Kajita, H.; Muraki, N.; Oda, Y.; Satoh, S.; Tsukamoto, Y.; Kimura, S.; Onoue, K.; Yonemura, S.; Arakawa, S.; Kato, H.; Hirashima, T.; Kawane, K. Apoptotic extracellular vesicle formation via local phosphatidylserine exposure drives efficient cell extrusion. *Dev. Cell* **2023**, *58*, 1282–1298.
44. MacDonald, J.M.; Beach, M.G.; Porpiglia, E.; Sheehan, A.E.; Watts, R.J. Freeman, M.R. The *Drosophila* cell corpse engulfment receptor Draper mediates glial clearance of severed axons. *Neuron* **2006**, *50*, 869–881.
45. Badinloo, M.; Nguyen, E.; Suh, W.; Alzahrani, F.; Castellanos, J.; Klichko, VI.; Orr,WC.; Radyuk, SN. Overexpression of antimicrobial peptides contributes to aging through cytotoxic effects in *Drosophila* tissues. *Arch. Insect. Biochem. Physiol.* **2018**, *98*, e21464.
46. Sapar, M.L.; Ji, H.; Wang, B.; Poe, A.R.; Dubey, K.; Ren, X.; Ni, J.Q.; Han, C. Phosphatidylserine externalization results from and causes neurite degeneration in *Drosophila*. *Cell Rep.* **2018**, *24*, 2273–2286.
47. Oka, S.; Hirai, J.; Yasukawa, T.; Nakahara, Y.; Inoue, Y.H. A correlation of reactive oxygen species accumulation by depletion of superoxide dismutases with age-dependent impairment in the nervous system and muscles of *Drosophila* adults. *Biogerontol.* **2015**, *16*, 485–501.
48. Reimels, TA.; Pfleger, CM. Methods to examine the lymph gland and hemocytes in *Drosophila* larvae. *J. Vis. Exp.* **2016**, *117*, 54544.
49. Evans, C. J.; Hartenstein, V.; Banerjee, U. Thicker than blood: conserved mechanisms in *Drosophila* and vertebrate hematopoiesis. *Dev. Cell* **2003**, *5*, 673–690.
50. Jung, S.-H.; Evans, C. J.; Uemura, C.; Banerjee, U. The *Drosophila* lymph gland as a developmental model of hematopoiesis. *Development* **2005**, *132*, 2521–2533.
51. Anghel, R.; Jitaru, D.; Bădescu, L.; Bădescu, M.; Ciocoiu, M. The cytotoxic effect of magainin II on the MDA-MB-231 and M14K tumour cell lines. *Biomed. Res. Int.* **2013**, *2013*, 831709.
52. Shiomi, A.; Nagao, K.; Yokota, N.; Tsuchiya, M.; Kato, U.; Juni, N.; Hara, Y.; Mori, MX.; Mori, Y.; Ui-Tei, K.; Murate, M.; Kobayashi, T.; Nishino, Y.; Miyazawa, A.; Yamamoto, A.; Suzuki, R.;

Kaufmann, S.; Tanaka, M.; Tatsumi, K.; Nakabe, K.; Shintaku, H.; Yesylevsky, S.; Bogdanov, M.; Umeda, M. Extreme deformability of insect cell membranes is governed by phospholipid scrambling. *Cell Rep*. **2021**, *35*, 109219.

53. Diefenbach, A.; Tomasello, E.; Lucas, M.; Jamieson, A. M.; Hsia, J. K.; Vivier, E.; Raulet, D. H. Selective associations with signaling proteins determine stimulatory versus costimulatory activity of NKG2D. *Nat. Immunol.* **2002**, *3*, 1142–1149.
54. Fridman, W.H.; Pagès, F.; Sautès-Fridman, C.; Galon, J. The immune contexture in human tumours: impact on clinical outcome. *Nat. Rev. Cancer.* **2012**, *12*, 298–306.
55. Schreiber, R.D.; Old. L.J.; Smyth, M.J. Cancer immunoediting: integrating immunity's roles in cancer suppression and promotion. *Science* **2011** *331*, 1565–1570.
56. Kalbasi, A.; June, C. H.; Haas, N.; Vapiwala, N. Radiation and immunotherapy: A synergistic combination. *J. Clin. Invest.* **2013**, *123*, 2756–2763.
57. Yoo, T.-J.; Sup Shim, M.; Bang, J.; Kim, J.-H.; Jae Lee, B. SPS1 deficiency-triggered *PGRP-LC* and *Toll* expression controls innate immunity in *Drosophila* S2 Cells. *Biol. Open* **2022**, *11*, bio059295.
58. Kinoshita, Y.; Shiratsuchi, N.; Araki, M.; Inoue, Y.H. Anti-tumor effect of Turandot proteins induced via the JAK/STAT pathway in the *mxc* hematopoietic tumor mutant in *Drosophila*. *Cells,* **2023**, *12*, 2047.
59. Jin X.; Mei H.; Li X.; Ma Y.; Zeng AH, Wang Y. Apoptosis-inducing activity of the antimicrobial peptide Cecropin of *Musca domestica* in human hepatocellular carcinoma cell line BEL-7402 and the possible mechanism. *Acta. Biochim. Biophys. Sin. (Shanghai)* **2010**, 259–265.
60. Sang, M.; Zhang, J.; Zhuge, Q. Selective cytotoxicity of the antibacterial peptide ABP-dHC-Cecropin A and its analog towards leukemia cells. *Eur. J. Pharmacol*. **2017**, *803*, 138–147.
61. Zhang, L.; Gallo, R.L. Antimicrobial peptides. *Curr. Biol.* **2016**, 26, R14–R19.
62. Brady, D.; Grapputo, A.; Romoli, O.; Sandrelli, F. Insect Cecropins, antimicrobial peptides with potential therapeutic applications. *Int. J. Mol. Sci.* **2019**, *20*, 5862.
63. Ziaja, M.; Dziedzic, A.; Szafraniec, K.; Piastowska-Ciesielska, A. Cecropins in cancer therapies-where we have been? *Eur. J. Pharmacol.* **2020**, *882*, 173317.
64. Hoskin, D. W.; Ramamoorthy, A. Studies on anticancer activities of antimicrobial peptides. *Biochim. Biophys. Acta, Bioenerg.* **2008**, *1778*, 357–375.
65. Serizier, S.B.; Peterson, J.S.; McCall, K. Non-autonomous cell death induced by the Draper phagocytosis receptor requires signaling through the JNK and SRC pathways. *J. Cell Sci.* **2022** *135*, jcs250134.
66. Bonifacino, J. S.; Glick, B. S. The mechanisms of vesicle budding and fusion. *Cell* **2004**, *116*, 153–166.
67. Shandala, T.; Brooks, D. A. Innate immunity and exocytosis of antimicrobial peptides. *Commun. Integr. Biol.* **2012**, *5*, 214–216.
68. O'Sullivan, M.J.; Lindsay, A.J. The endosomal recycling pathway-at the crossroads of the cell. *Int. J. Mol. Sci.* **2020**, *21*, 6074.
69. Thorn, P.; Zorec, R.; Rettig, J.; Keating, D.J. Exocytosis in non-neuronal cells. *J Neurochem.* **2016**, *137*, 849–859.
70. Schweizer F. Cationic amphiphilic peptides with cancer-selective toxicity. *Eur. J. Pharmacol.* **2009**, *625*, 190–194.
71. Daleke, D. L. Phospholipid flippases. *J. Biol. Chem.* **2007**, *282*, 821–825.
72. Bevers, E. M.; Williamson, P.L. Phospholipid scramblase: an update. *FEBS Lett.* **2010**, *584*, 2724–

 doi:10.20944/preprints202501.2343.v1

2730.

73. Iwasaki, T.; Ishibashi, J.; Tanaka, H.; Sato, M.; Asaoka, A.; Taylor, D.; Yamakawa, M. Selective cancer cell cytotoxicity of enantiomeric 9-Mer peptides derived from beetle Defensins depends on negatively charged phosphatidylserine on the cell surface. *Peptides* **2009**, *30*, 660–668.
74. Mader, J. S.; Hoskin, D.W. Cationic antimicrobial peptides as novel cytotoxic agents for cancer treatment. *Expert. Opin. Investig. Drugs* **2006**, *15*, 933–946.
75. Riedl, S.; Rinner, B.; Asslaber, M.; Schaider, H.; Walzer, S.; Novak, A.; Lohner, K.; Zweytick, D. In Search of a Novel Target — Phosphatidylserine exposed by non-apoptotic tumor cells and metastases of malignancies with poor treatment efficacy. *Biochimi. Biophys. Acta, Biomembr.* **2011**, *1808*, 2638–2645.
76. Gao, X.; Ding, J.; Liao, C.; Xu, J.; Liu, X.; Lu, W. Defensins: The natural peptide antibiotic. *Adv. Drug Deliv. Rev.* **2021**, *179*, 114008.